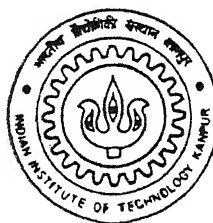


Computer Aided Synthesis, Analysis and Animation of Planar Six-Bar Linkages

by

S. Neeraj



DEPARTMENT OF MECHANICAL ENGINEERING
INDIAN INSTITUTE OF TECHNOLOGY KANPUR

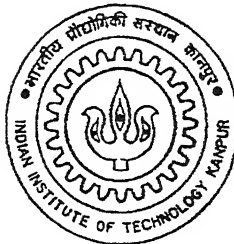
April, 1999

Computer Aided Synthesis, Analysis and Animation of Planar Six-Bar Linkages

*A Thesis Submitted
in Partial Fulfilment of the Requirements
for the Degree of
Master of Technology*

by

S. Neeraj



*to the
DEPARTMENT OF MECHANICAL ENGINEERING
INDIAN INSTITUTE OF TECHNOLOGY, KANPUR*

April, 1999

31 MAY 1000 ME
CENTRAL LIBRARY
FEDERAL REPUBLIC
No. A 128072

TM
MESSAGE
MESSAGE

To the memory of my beloved Nanaji

Late. Shri V. Rajagopala Iyer

who was known as Doctor of Machines during his Textile Mill days

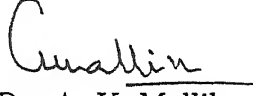
To the process of

Creativity

which brings something into new being

CERTIFICATE

It is certified that the work contained in the thesis entitled **Computer Aided Synthesis, Analysis and Animation of Planar Six-Bar Linkages** by S. Neeraj, has been carried out under my supervision and this work has not been submitted elsewhere for a degree.


Dr. A. K. Mallik

Thesis Supervisor

Department of Mechanical Engineering

I. I. T. Kanpur

Acknowledgements

I owe a deep debt of gratitude, respect and love to Mallik Sir, whose guidance and encouragement made me accomplish this work successfully. He is more than a Professor to me - He is a Teacher who taught me to understand knowledge in its correct perspective. I enjoyed the care and affection he showered on me. During the entire work he allowed me to work at my leisure. He never set any deadlines for me and I never failed to use this undue privilege. I learnt many things from him - Dynamics, Mechanisms and a positive attitude towards life. The only thing he never taught me was 'Computers'. I pray to God for his health and hope for a continuing relationship with him. Working with him is a memorable experience for me.

I am grateful to Dr. Sudipto Mukherjee for his guidance in the programming part of the thesis. I take this opportunity to appreciate Mr. Niteesh, Gaurav, Ishan and Vishesh for the wonderful work they have done in the project. They always helped me whenever I got stuck in the programming.

I would like to acknowledge Anjanda for his help and suggestions in 'Optimizing Techniques' in the thesis. Deep thanks goes to Santosh Kulloo without whose great help I would never have been able to write my report.

Warm appreciation and regards are for Goutamda, who always bore my numerous queries and who was most of the time the first person to whom I would show my results. In addition I would like to thank all the members of the Vibrations and Dynamics Lab. I will always remember the rides on the cycle with Yogesh during which we discussed whatnot. I acknowledge my room partner Amreesh who was always there to encourage me. Appreciation goes to Asit and Sandeep with whom I spent a major part of my time. Thanks to Amit and Dhish for their ever supportive attitude. I thank Anya, Ganesh, Santosh, Subodh, Suma, Yogya and the whole Ghati Mandal for their affection towards me. I will always cherish the lighter moments of life I shared with Anjanda. Friendship with Arvind, Chandu, Jeyakumar, L.Shree, Santosh Kalva, Lt. Sanjay, Venkat, Shastriji is just a begin-

ning.

I will always remember my cute Samtron terminal.

I wish to express my unbounded love for my Naniji, Ma, Daddy and Bhai.

Stay at I.I.T. was a very beautiful and important phase of my life.

Neeraj

Abstract

Many software packages are available for design of mechanisms. Using computers, a designer can solve complex and practical problems rapidly and at the same time can also test a vast spectrum of alternatives.

The main objective of the present thesis, as a part of DST sponsored project, is to develop a methodology for computer aided design of Planar Six-Bar Linkages. The software package developed provides all the facilities of analysis and animation as well.

The use of various optimization techniques in synthesis problems results in satisfactory solutions. The Least Square Error Minimizing Technique has been used which does not involve the time consuming iterations. Non-linearity in the design equations is resolved using Linear Superposition Technique. Examples are included to show the practical application of the synthesis methods. Computer programs have been developed using C++ (Borland 4.5 with graphics facilities).

Contents

Certificate	i
Acknowledgements	ii
Abstract	iv
List of Figures	vii
List of Tables	ix
List of Symbols	xii
1 Introduction	1
1.1 Introduction	1
1.2 Objectives and Scope of the Present Work	3
2 Planar Six-Bar Linkages	5
2.1 Introduction	5
2.2 Classification of Planar Six-Bar Linkages	6
2.3 Applications of Planar Six-Bar Linkages	7
2.3.1 Stephenson's Linkage	7
2.3.2 Watt's Linkage	8
2.4 Other Examples and Applications	9

3 The Least Square Error Method and the Linear Superposition Technique	13
3.1 Methods of Linkage Synthesis	13
3.2 Least Square Error Method (LSM)	14
3.3 The Linear Superposition Technique	15
3.4 Use in Linkage Synthesis	17
4 Synthesis of Planar Six-Bar Linkages	18
4.1 Classification of Synthesis Problems	18
4.2 Function Generation using Stephenson-I Linkage	19
4.3 Path Generation using Stephenson-I Linkage	23
4.4 Motion Generation using Watt-II Linkage	28
4.5 Numerical Examples	32
4.6 Conclusions	38
5 Optimization of Transmission Angle for Planar Four-Bar Linkages	46
5.1 Introduction	46
5.2 Transmission Angle	46
5.3 Optimization for Function Generation	47
5.4 Optimization for Path Generation	53
5.5 Numerical Examples	55
5.6 Conclusion	57
6 Conclusions	64
6.1 Suggestions for Future Work	66
Bibliography	67
Appendix A	69

List of Figures

2.1	Stephenson's chain	6
2.2	Watt's chain	6
2.3	One revolution of drive crank AB produces two oscillations of output link ED .	9
2.4	Crank ED drives the rocking four-bar $ABGF$, through the coupler point C .	10
2.5	Large angle of oscillation θ_{AB}^{12} of rocker AB corresponds to angle θ_{ED}^{12} of crank ED .	10
2.6	Revolving link ED dwells three times during its rotation, in one rotation of driving crank AB .	11
2.7	Output link ED dwells when coupler point C traverses the circular path C_1C_2 .	11
2.8	Stephenson-I linkage with a rocker having a swing angle more than 360° in one direction.	12
2.9	Watt's linkage to satisfy the spacing requirement.	12
4.1	Stephenson-I as Function Generator.	19
4.2	Link-vector diagram of Stephenson-I at the i^{th} design position for function generation.	20
4.3	Stephenson-I, as Path Generator, at the i^{th} design position when generating a path.	24
4.4	Watt-II, as Motion Generator, at the i^{th} design position generating rigid-body motion.	29

4.5	Stephenson-I linkage optimized in Example 2 to generate an output rocking angle of more than 180° with a rotary input.	34
4.6	Page turning linkage.	35
4.7	Stephenson-I linkage optimized in Example 3 to generate path for the page turning linkage.	36
4.8	The available space inside the garage is determined by the envelope of the straight lines, representing the garage-door at various positions.	37
4.9	Watt-II linkage optimized in Example 4 to guide the garage-door.	37
5.1	Transmission angle μ of a four-bar linkage.	47
5.2	Transmission angle μ as the acute angle between link 3 and link 4.	48
5.3	Four-bar linkage at the i^{th} design position when generating a function.	48
5.4	Four-bar linkage at the i^{th} design position when generating a path.	53
5.5	Four-bar linkage synthesized in Example 2 for path generation.	57

List of Tables

Table 4.1	Desired displacements for the function ($y = x^2$, $-1 \leq x \leq +1$) for which the Stephenson-I linkage is optimized in Example 1.	39
Table 4.2	Desired and generated displacements for the Stephenson-I linkage in Example 1 for function generation. $\Delta\theta_{12} = 90^\circ$, $\Delta\theta_{41} = 60^\circ$	39
Table 4.3	Generated displacements for the Stephenson-I linkage in Example 1 when $(\theta_{5ai})_g$ of Table 4.1 are used as input values.	40
Table 4.4	Desired and generated displacements for the Stephenson-I linkage in Example 2 for an output oscillation of more than 180°	40
Table 4.5	Generated displacements for the Stephenson-I linkage in Example 2 when $(\theta_{5ai})_g$ of Table 4.4 are used as input values.	41
Table 4.6	Desired and generated co-ordinates of the path for the Stephenson-I linkage in Example 3.	41
Table 4.7	Generated displacements for the Stephenson-I linkage in Example 3 for path generation.	42
Table 4.8	Desired and generated co-ordinates of the path for the Watt-II linkage in Example 4 for motion of the garage-door.	42
Table 4.9	Generated displacements for the Stephenson-I linkage in Example 3 for path generation.	43

Table 4.10 Generated co-ordinates of the path for the Watt-II linkage in Example 4 for motion of the garage-door, with $L_{5b} = 0$ cm.	43
Table 4.11 Generated displacements for the Watt-II linkage in Example 4 for motion of the garage-door, with $L_{5b} = 0$ cm.	44
Table 5.1 Desired and generated displacements for the four-bar linkage in Example 1 for function generation.	57
Table 5.2(a) Generated displacements for the four-bar linkage in Example 1 obtained using Cauchy's steepest descent method for $\mu_{min} = 20^\circ$	57
Table 5.2(b) Generated displacements for the four-bar linkage in Example 1 obtained using Cauchy's steepest descent method for $\mu_{min} = 25^\circ$	58
Table 5.2(c) Generated displacements for the four-bar linkage in Example 1 obtained using Cauchy's steepest descent method for $\mu_{min} = 30^\circ$	58
Table 5.3(a) Generated displacements for the four-bar linkage in Example 1 obtained using Random search method for $\mu_{min} = 20^\circ$	59
Table 5.3(b) Generated displacements for the four-bar linkage in Example 1 obtained using Random search method for $\mu_{min} = 25^\circ$	59
Table 5.4 Desired and generated displacements for the four-bar linkage in Example 2 for path generation.	60
Table 5.5(a) Generated displacements for the four-bar linkage in Example 2 obtained using Cauchy's steepest descent method for $\mu_{min} = 25^\circ$	60
Table 5.5(b) Generated displacements for the four-bar linkage in Example 2 obtained using Cauchy's steepest descent method for $\mu_{min} = 30^\circ$	61

Table 5.6(a) Generated displacements for the four-bar linkage in Example 2 obtained using Random search method for $\mu_{min} = 25^\circ$ 61

Table 5.6(b) Generated displacements for the four-bar linkage in Example 2 obtained using Random search method for $\mu_{min} = 30^\circ$ 62

List of Symbols

\vec{d}	Length vector showing position of a coupler point on the floating link
e_i	Error in the generated function at the i^{th} design position
e_{avg}, e_{rms}	Average and root-mean-square value of the error in the generated function
L_j	Length of the j^{th} link of planar four-bar linkage
L_j	Length of the j^{th} link of planar six-bar linkage
\vec{P}_i	Position vector of the i^{th} design point on the path to be generated
\vec{R}_J	Position vector of the fixed hinge J of the linkage
α_J	Angle made by \vec{R}_J with the horizontal axis
β_i	Angle used in calculation for synthesis at the i^{th} design position
γ_c	Angular dimension of ternary link 5 of the six-bar linkage
δ_i	Angle made by \vec{P}_i with the horizontal axis
ϵ	Angle made by (a line on) a rigid body with respect to the carrier link
η_c	Angular dimension of ternary link 6 of the six-bar linkage
θ_{ji}	Angle made by link L_j of four-bar linkage with the horizontal axis at the i^{th} design position

θ_{jki}	Angle made by link L_{jki} of six-bar linkage with the horizontal axis at the i^{th} design position
λ	Non-linearity coefficient
μ	Transmission angle of four-bar linkage
μ_1, μ_2	Transmission angles of six-bar linkage
ξ_i	Angle made by (a line on) a rigid-body with the horizontal axis at the i^{th} design position
ψ	Angle made by $\vec{\alpha}$ with the floating link

Chapter 1

Introduction

1.1 Introduction

A mechanism is a device that serves the purpose of transferring motion and/or force from a source to an output member. Mechanisms have been devised and used since the dawn of human civilization. From the modest beginning with wheel and pulley (on an axle), the lever and the gear, through the sewing machine and the typewriter, up to the most modern aircrafts and ships, the development has been tremendous.

The early designs were totally based on imagination and intuition. The Industrial Revolution provided great impetus to mechanism design. Steam engines and weaving looms came into existence. However, it was not until the end of 19th century that a more systematic study of mechanisms started with “Theorestische Kinematic” by Reauleaux in 1875. Since then the mechanism design has taken the form of a well established subject. Later on, various machine tools, textile and other heavy machinery such as bulldozers, lift-jacks and construction machines were also developed with the aid of ever increasing research in theory and operations of mechanisms. The mechanism design did not remain limited to the heavy machine industries only. The fields of photographic instruments, clocks, artificial limbs and mechanical toys also saw newer and improved designs at the

same time.

The 1950s saw the introduction of digital computers. The advent of computers in the field of engineering, revolutionized the mechanism design. The speed and computational capabilities of computers rendered complex design calculations feasible and economical, thus giving birth to **Computer Aided Mechanism Design (CAMD)**.

The graphical techniques of mechanism analysis and synthesis as well as animation were brought under the ambit of CAMD as soon as graphics packages became available. The arduous task of repetitive designs to choose the better one has been rendered simple with CAMD. Also newer synthesis techniques, using various optimization methods, were developed to solve complicated problems.

During the last 30 years, many CAMD packages have been developed. The earliest packages were KINSYN and LINCAGES. After these came IMP, DRAM, ADAMS, MCADA, DADS and many others. All these packages have been quite popular in academic institutions as well as in the industry. The reason for their popularity can be attributed to the fact that CAMD enables the designer to use his creativity to full extent, which lifts the limitation on imagination leading to better and useful designs. Writing about KINSYN, Kaufman commented

"In order to innovate freely in the field of kinematics, one should be unencumbered by time - consuming and distracting analytical procedures. Ideally a designer should be able to envision a new device and "presto"! Instantly a machine shop model materializes in his hands, one that he can handle, massage, rock back and forth, wiggle and contemplate; a model whose dimensions are plastic, so that he can push and pull it into new shapes, modeling it until its behavior is just right; a model whose topology is flexible, so that he can study the effects of changing a slider to a hinge, or a cam to a linkage." (Kaufman, R. E., *Mechanism and Machine Theory*, 1973, Vol. 8, p. 470)

The objective of the present thesis is to prepare a software package, as a part of DST

sponsored project, for dimensional synthesis, analysis and animation of Planar Six-Bar Linkages.

A mechanism which has got all the joints as lower pairs is commonly called a *linkage*. In a planar linkage, all the links move in planes that remain parallel to each other, and the axes of all revolute pairs also remain parallel to each other.

Dubey [1] has prepared a software package under the same project which focuses on planar four-bar linkages. That package provides the tools to carry out the dimensional synthesis, analysis and animation of planar four-bar linkages. The synthesis is based on two approaches, viz., the precision-point technique and the optimization technique. The user has got the choice of using any of the two approaches.

1.2 Objectives and Scope of the Present Work

The planar six-bar linkage is a single degree of freedom linkage. It is used in situations where a planar four-bar linkage fails to satisfy the kinematic requirements.

The primary objective of the present thesis is to develop a computer aided design methodology for planar six-bar linkages for the purpose of function generation, path generation and motion generation. The analysis and the animation of the linkages are also made available to check the functioning of the linkages so designed.

In Chapter 2, different types of planar six-bar linkages are considered. The different linkages that can be obtained from planar six-bar chain by fixing one link at a time, are discussed. Some examples of typical applications are mentioned.

A number of optimization methods are available for linkage synthesis. The present work uses the **Least Square Error Minimizing Optimization Technique**, more popularly known as **Least Square Method (LSM)**. Chapter 3, starts with a brief discussion on the available methods of linkage synthesis. It explains the LSM in detail. The planar six-bar linkage is a multi-loop linkage. The dimensions of the optimum linkage are determined

by minimizing the error in the loop-closure equation of each loop of the linkage. The multi-loop linkage gives rise to nonlinear equations which are formed as linear equations using the **Linear Superposition Technique**. The linear superposition technique is also explained in Chapter 3.

The mathematical background of the synthesis procedure is outlined in Chapter 4. The optimum synthesis of Stephenson-I type linkage for Function Generation and Path Generation and optimum synthesis of Watt-II type linkage for Motion Generation are detailed.

In Chapter 5, the optimization of transmission angle of planar four-bar linkage for Function Generation and Path Generation is given. This is an extension of the work done by Dubey [1].

The main conclusions of the present work are summarized in Chapter 6. Some directions for future work are also mentioned therein.

Appendix A, gives the description of the tools of analysis and synthesis that the present software package provides.

To meet the computational and animation requirements, C++ (Borland 4.5 with graphics facility) on DOS platform was selected as the programming language.

The development of the package and hence the project has been done with the aim that the computer should accept performance specifications of the linkages in the user's terms. The user should be able to test alternatives and carry out the detailed analysis processes without worrying about the calculations involved. At the same time, it should not be expected that for any given data, not in compliance with equations involved, the package will produce a satisfactory result. The package should be useful in both academic institutions and industry.

Chapter 2

Planar Six-Bar Linkages

2.1 Introduction

The four-bar linkage has the least possible number of links of all the planar linkages. Over the last 100 years, various graphical and analytical techniques have been developed for its analysis and dimensional synthesis. The literature is very rich with numerous uses and examples of four-bar linkage. Still, sometimes it happens that a four-bar linkage does not provide the required level of performance needed for a particular application. In some applications a four-bar linkage fails completely. This is where the designer resorts to planar six-bar linkages.

A six-bar linkage has more complex motion relationships among its links as compared to a four-bar linkage. Such complex relationships, either can not be fulfilled, or can only be partially fulfilled, by a four-bar linkage. Sometimes the four-bar linkage may satisfy the required kinematic objectives, but then its transmission quality may turn out to be too poor.

2.2 Classification of Planar Six-Bar Linkages

From Grübler's criterion, it can be easily shown that a planar six-bar linkage must have four binary and two ternary links. Two different arrangements are possible. In one arrangement (Figure 2.1), two ternary links are connected by a binary link, which is known as *Stephenson's chain*. In the other arrangement (Figure 2.2), two ternary links are connected to each other, which is known as *Watt's chain*.

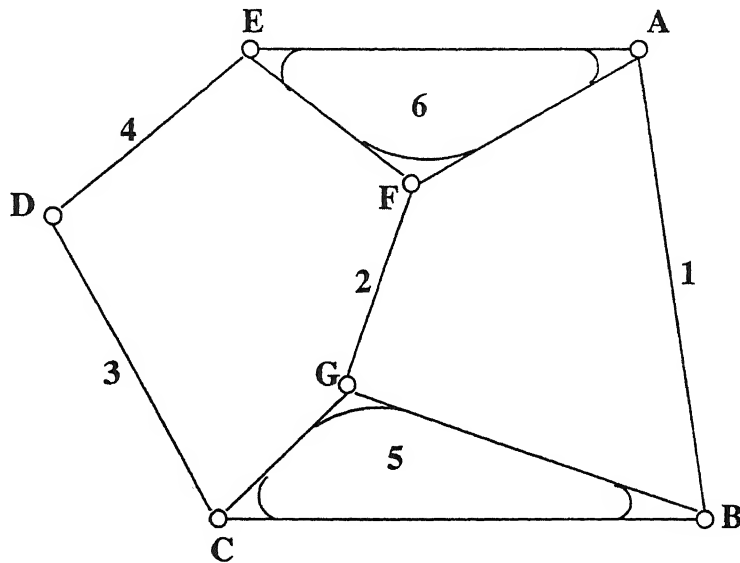


Figure 2.1: Stephenson's chain

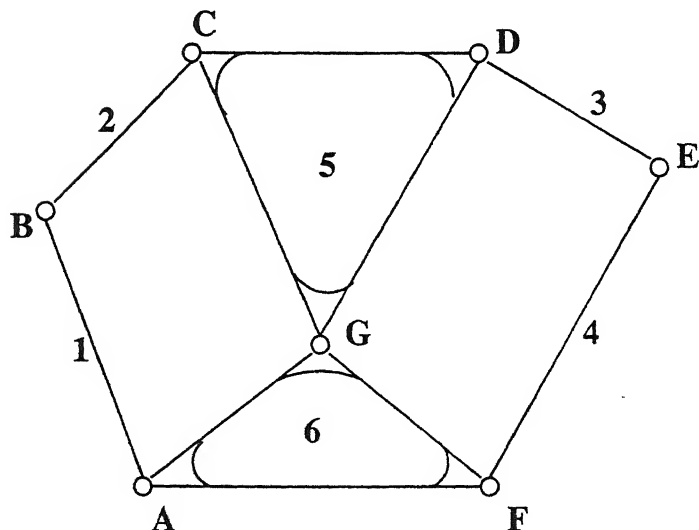


Figure 2.2: Watt's chain

By kinematic inversion, three different types of linkages are obtained from a Stephenson's chain. *Stephenson-I* is obtained by fixing one of the ternary links (5 or 6 in Figure 2.1). *Stephenson-II* is obtained by fixing one of the binary links that are connected to each other (3 or 4 in Figure 2.1). *Stephenson-III* is obtained by fixing one of the binary links that are connected to the two ternary links at both ends (1 or 2 in Figure 2.1).

Two different types of linkages are obtained by kinematic inversions of Watt's chain. *Watt-I* is obtained if one of the ternary links is fixed (5 or 6 in Figure 2.2). If any of the four binary links is fixed (1, 2, 3 or 4 in Figure 2.2) *Watt-II* is obtained.

2.3 Applications of Planar Six-Bar Linkages

Some typical examples of planar six-bar linkages are covered in this section, which bring out their distinct applications.

2.3.1 Stephenson's Linkage

This linkage is generally used for the following purposes:

1. For output link oscillation with double or triple advance and return during one revolution of the input link. Figure 2.3 shows that output link ED oscillates twice during one revolution of the drive crank AB (Hain [2], pp. 383-5). The coupler curve generated by the coupler point C is indicated by α in the figure.
2. For driving the two rocker links of a four-bar linkage, with a continuous crank rotation. Figure 2.4 shows that the revolving crank ED , via link DC , drives the double rocker linkage $ABGF$ (Hain [2], pp. 386-7).
3. For large angle of output oscillation. In Figure 2.5, crank ED makes output link AB to oscillate through 180° (Hain [2], pp. 390-1).

4. For producing dwell, where the output link remains stationary (at least approximately) during continuous motion of the input link. Figure 2.6 shows that link ED has a continuous rotary motion with three dwells per revolution, with link AB as the driving crank (Hain [2], pp. 391-2). Figure 2.7 shows a linkage in which the output link ED dwells when the coupler point moves through the portion of the coupler curve having almost constant radius of curvature (Tao [3], p. 80).
5. For producing a unidirectional output-link oscillation of more than 360° with a continuous rotary input (Shukla and Mallik [15]). It is seen from Figure 2.8, that clockwise rotation of crank BA produces oscillation of link CD of 14.5° in clockwise direction and 374.5° in counterclockwise direction.

2.3.2 Watt's Linkage

This linkage is used for the following purposes:

1. For obtaining a large oscillation angle of the output link from a small input link angle or vice versa. Figure 2.9 shows that the difference in lengths of the two arms of the link CGD will amplify or reduce the curvilinear displacement of the input GD of the second four-bar linkage $GDEF$ thus directly varying the output angle θ_{OUT} (Tao [3], pp. 24-5).
2. For obtaining a more suitable practical design. As can be seen from Figure 2.9, if the given hinges A and F are too far apart for a single, sturdy four-bar linkage, a six-bar linkage can be designed by suitably choosing the intermediate fixed pivot G (Tao [3], pp. 24-6).

2.4 Other Examples and Applications

Many more examples and applications of planar six-bar linkage using its complicated motion transfer characteristics are given by Hain [2], Tao [3] and Hunt [4]. Erdman and Sandor [5] (Vol. I, pp. 11-5) gives some typical examples of six-bar linkage as a tape carrier linkage in cassette player and as a prosthesis knee mechanism. Mallik et al [6] gives the examples of parallel-jaw pliers (pp. 364-7), fork lifter without a vertical guide (pp. 254-8), and Hart's straight line mechanism (pp. 372-3). These linkages are obtained from Watt's chain.

The purpose of inclusion of these examples in this chapter is to show the advantages of six-bar linkages over four-bar linkages. In all the cases considered, the four-bar linkage would have failed to perform satisfactorily. Yet, it is worth mentioning that most of the above examples have the origin of their design in four-bar planar linkages only. The details of the design and synthesis can be obtained from the references.

The planar six-bar linkage has been a topic of research since 1950s; still a long way is to be covered to understand it completely.

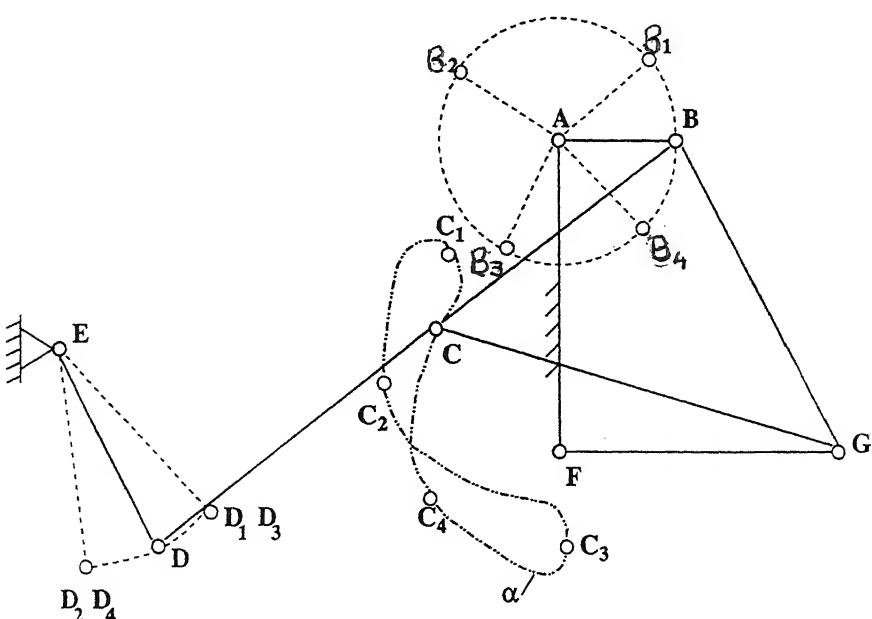


Figure 2.3: One revolution of drive crank AB produces two oscillations of output link ED .

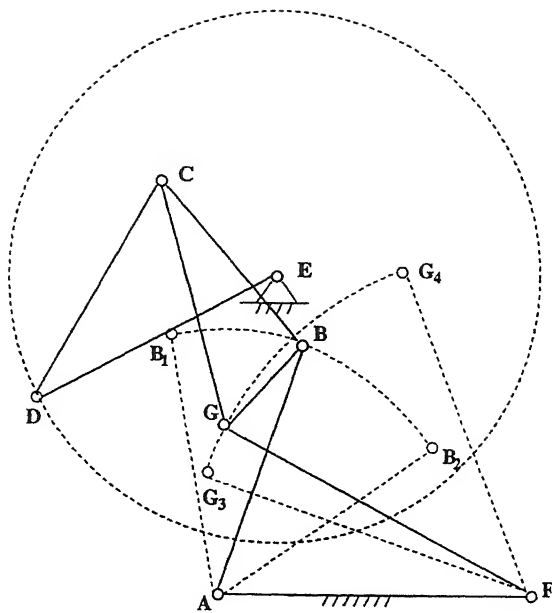


Figure 2.4: Crank ED drives the rocking four-bar $ABGF$, through the coupler point C .

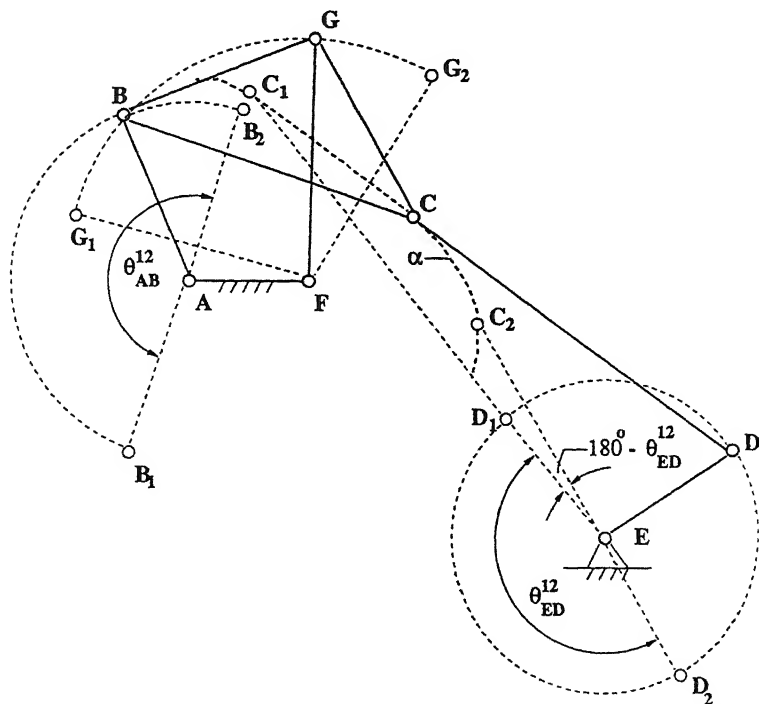


Figure 2.5: Large angle of oscillation θ_{AB}^{12} of rocker AB corresponds to angle θ_{ED}^{12} of crank ED .

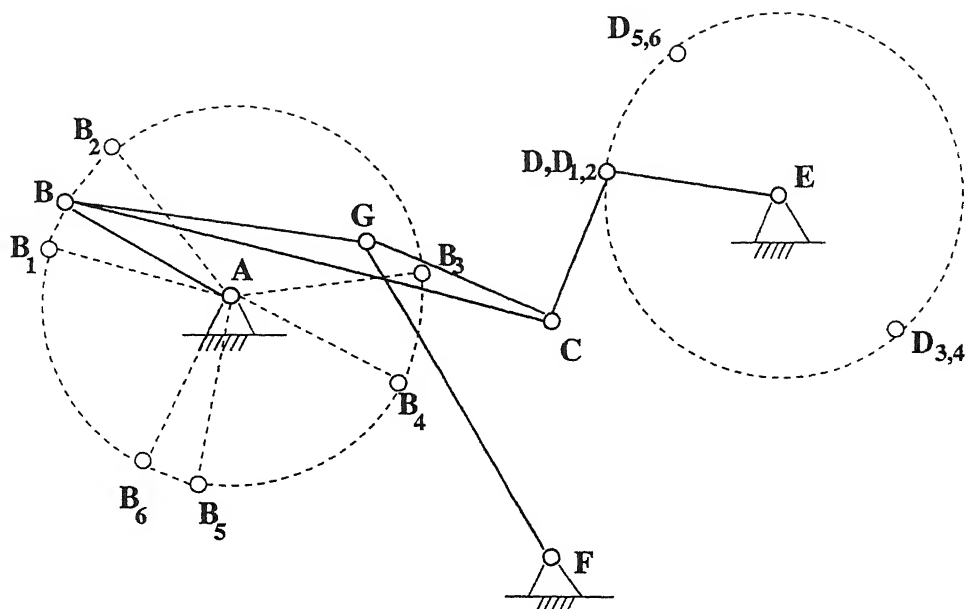


Figure 2.6: Revolving link ED dwells three times during its rotation, in one rotation of driving crank AB .

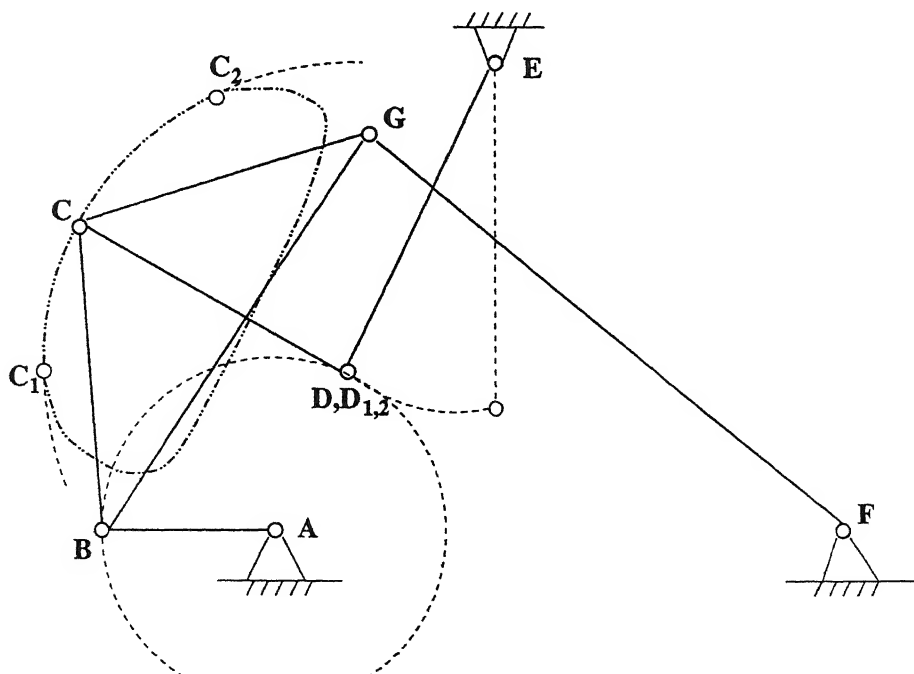


Figure 2.7: Output link ED dwells when coupler point C traverses the circular path C_1C_2 .

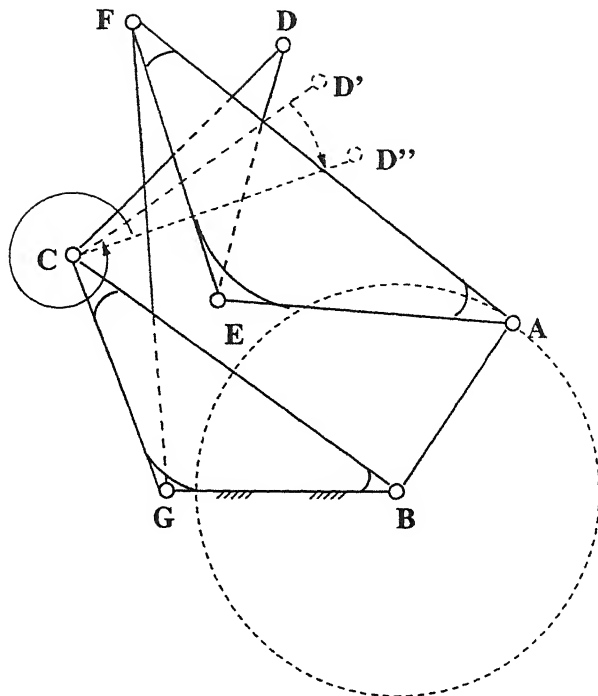


Figure 2.8: Stephenson-I linkage with a rocker having a swing angle more than 360° in one direction.

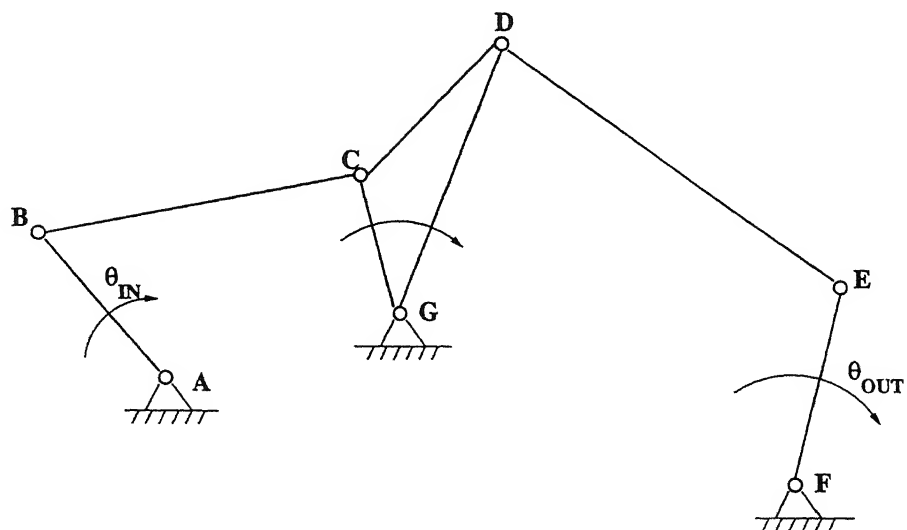


Figure 2.9: Watt's linkage to satisfy the spacing requirement.

Chapter 3

The Least Square Error Method and the Linear Superposition Technique

3.1 Methods of Linkage Synthesis

Research in linkage synthesis is being carried out on two broad fronts - (a) Precision point synthesis, and (b) Application of mathematical programming techniques.

In the precision point approach, a linkage is obtained which can generate a function, path or motion with exact accuracy at a limited number of discrete points. But at remaining configurations there exists some difference between the desired and generated characteristics which is called the structural error. The precision points are selected so as to minimize the maximum structural error. The number of precision points is limited by the number of design parameters. Mallik et al [6] and Hartenberg and Denavit [7] can be referred to for detailed procedure of precision point synthesis. McLarnan [8] has dealt with precision point synthesis of planar six-bar linkages for function generation.

The application of mathematical programming techniques to linkage synthesis provides a method in which the structural error, which may not be zero anywhere, is minimized in an overall sense in the entire range of motion of the linkage. Any number of design points¹

¹The points should not be called precision points.

are chosen and some error quantity or function, suitably defined, using these chosen points is minimized. The error quantity or function is constructed using the difference between the actual and desired linkage characteristics. The number of design points is not limited by the number of available design parameters. The optimization technique to be used for minimizing the error can be **Least Square Error method (LSM)**, Galerkin's method, Cauchy's steepest descent method or Random search method.

Of all these methods the least square error method has some advantages. The problem formulation is very straight forward and the solution procedure is not based on time consuming iterations. The nonlinear objective equations can be linearized using the **Linear Superposition Technique**. The Least Square Error Method and the Linear Superposition Technique are explained in detail in the sections to follow.

Fox and Gupta [9] provides a review and summary of the relationship between optimization methods (mathematical programming) and mechanism synthesis. It also gives a bibliography on the subject.

3.2 Least Square Error Method (LSM)

The method is one of the most popular methods of numerical techniques. In this method, the sum of squares of deviations of actual values from the desired values at some number of chosen points is minimized.

The method can be clearly explained by taking an example. A simple linear equation of two variables x and y is considered. Suppose the equation is given as

$$ax + by + k = 0 \quad (3.1)$$

and is to be fit through a given set of data points $(x_1, y_1), (x_2, y_2), \dots, (x_N, y_N)$. The unknowns are a and b ; k is some known constant. N can have any integral value ≥ 2 . Ideally, values of a and b should be such that at each given point, the left hand side of the equation

should give a value of zero, but actually at almost all points it will give a non zero value, say e , which is called the error at that point. For the error to be equally distributed the sum of errors at each design point, i.e., $e_1^2 + e_2^2 + \dots + e_N^2$ is minimized with respect to a and b . Writing in mathematical terms,

$$\begin{aligned} \frac{\partial}{\partial a} (e_1^2 + e_2^2 + \dots + e_N^2) &= 0 \\ \Rightarrow \frac{\partial}{\partial a} \left(\sum (ax + by + k)^2 \right) &= 0 \\ \Rightarrow a \sum x^2 + b \sum xy + k \sum x &= 0 \end{aligned} \tag{3.2}$$

similarly,

$$\begin{aligned} \frac{\partial}{\partial b} (e_1^2 + e_2^2 + \dots + e_N^2) &= 0 \\ \Rightarrow \frac{\partial}{\partial b} \left(\sum (ax + by + k)^2 \right) &= 0 \\ \Rightarrow a \sum xy + b \sum y^2 + k \sum y &= 0 \end{aligned} \tag{3.3}$$

Equations (3.2) and (3.3) form a set of simultaneous linear equations which can be solved by various methods like *Gauss Elimination method* etc., to give the values of a and b .

3.3 The Linear Superposition Technique

The equation considered in the previous section, i.e., Equation (3.1) is a linear equation. If the equation has a nonlinear term, then LSM can not be applied directly. For example, an equation with a nonlinear term is taken as

$$ax + by + abk_1 + k_2 = 0 \tag{3.4}$$

and the same N data points are to be used. k_1 and k_2 are some constants. The term ab brings nonlinearity in the equation. The linear superposition theory, as put forward by Bagci and Lee [10], partitions the above nonlinear equation into two linear equations. This is shown in the following steps. The term ab is represented by a so-called nonlinearity coefficient λ , i.e.

$$ab = \lambda. \quad (3.5)$$

Further, it is defined that

$$a = p_a + \lambda q_a \quad (3.6)$$

$$b = p_b + \lambda q_b \quad (3.7)$$

resulting in

$$(p_a + \lambda q_a)x + (p_b + \lambda q_b)y + \lambda k_1 + k_2 = 0$$

or

$$(p_a x + p_b y + k_2) + \lambda (q_a x + q_b y + k_1) = 0. \quad (3.8)$$

The above equation is partitioned into two linear equations as,

$$(p_a x + p_b y + k_2) = 0 \quad (3.9)$$

and

$$(q_a x + q_b y + k_1) = 0. \quad (3.10)$$

Both the resulting equations are solved using the LSM, giving values of (p_a, p_b) and (q_a, q_b) . The value of λ is obtained from Equations (3.5), (3.6) and (3.7) as,

$$(p_a + \lambda q_a) \times (p_b + \lambda q_b) = \lambda$$

or

$$\lambda^2 q_a q_b + \lambda (p_b q_a + p_a q_b - 1) + p_a p_b = 0. \quad (3.11)$$

The above quadratic equation, also known as the compatibility equation, is solved to obtain the value(s) of λ . No solution exists if the discriminant of Equation (3.11) turns out to be negative; a single value exists if it is equal to zero and two distinct solutions if it is greater than zero. Once λ is known, values of the original unknowns a and b are obtained from Equations (3.6) and (3.7).

3.4 Use in Linkage Synthesis

When the LSM is applied to Linkage Synthesis, the simple equations viz., Equations (3.1) and (3.4) are replaced by the loop closure equations. The unknowns, instead of a and b , are the dimensional parameters of the linkage. The data points are replaced by functions of the displacements which are to be generated by the linkage at the N design points (or positions). The error to be minimized is the sum of squares of error in the loop closure equations, at each design point.

Depending on the geometry and the number of unknown dimensions of the linkage, the loop closure equations may be linear or nonlinear. The nonlinearity is removed by using the linear superposition technique. The LSM results in simplified formulation and non iterative solution of the design equations.

The synthesis technique employing linear superposition has been applied to single-loop linkages for function generation [10], for path generation and rigid-body guidance (or motion generation) [11], and to multi-loop linkages for function generation [12] and for path generation and rigid-body guidance [13]. The present thesis presents the optimum synthesis techniques as applied to planar six-bar linkages for function generation, path generation and motion generation. The details of these are given in Chapter 4.

Chapter 4

Synthesis of Planar Six-Bar Linkages

4.1 Classification of Synthesis Problems

The present work focuses on dimensional synthesis of six-bar linkages. Dimensional synthesis involves the determination of link-lengths of a linkage so as to fulfill the prescribed motion characteristics. Depending on the motion characteristics to be satisfied, the synthesis problems can be classified as listed below:

1. *Function Generation:* In this type of problems, the motion parameters (displacement, velocity, acceleration etc.) of the output and input links are to be coordinated so as to satisfy a prescribed functional relationship.
2. *Path Generation:* Here a point on the floating link (i.e., a link not connected to the frame) of the linkage has to be guided along a prescribed path. The generation of the path may or may not be coordinated with the input motion.
3. *Motion Generation:* A rigid body (i.e., one link of the linkage) is guided in a prescribed manner. Here also the guidance may or may not be coordinated with the input motion.

The subsequent sections explain function generation and path generation for Stephenson-I and motion generation for Watt-II type linkages.

4.2 Function Generation using Stephenson-I Linkage

Figure 4.1 shows a Stephenson-I linkage. The input angle θ_{IN} represents the independent variable x , while the output angle θ_{OUT} represents the desired function $y = f(x)$. The link-vector diagram corresponding to Figure 4.1 is shown in Figure 4.2. The design variables are $L_{12}, L_{22}, L_{31}, L_{41}, L_{5a}, L_{5b}, L_{6a}, L_{6b}, \gamma_c$ and η_c ¹. The values of θ_{IN} and θ_{OUT} are represented, respectively, by θ_{12} and θ_{41} . The values of these angles at the N design points are evaluated using the prescribed function relationship, chosen scale factors (between x, y and θ_{12}, θ_{41}) and the respective initial values (of x, y and θ_{12}, θ_{41}). Out of the ten link design parameters, one link-length is arbitrarily chosen to fix the overall size of the linkage.

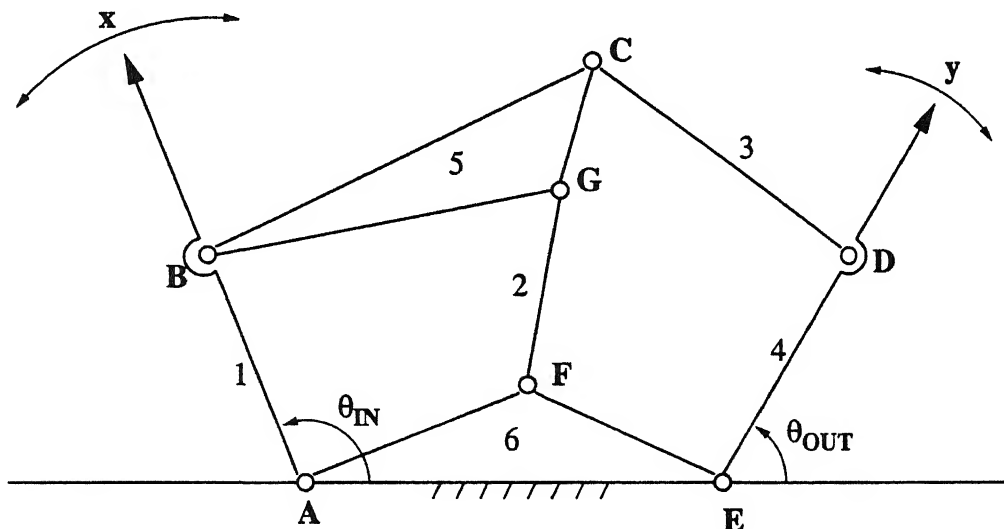


Figure 4.1: Stephenson-I as Function Generator.

For the loop $ABCDEA$, the loop closure equation is

$$\vec{L}_{12} + \vec{L}_{5b} + \vec{L}_{31} - \vec{L}_{6b} - \vec{L}_{41} = 0 \quad (4.1)$$

¹In all the sections of function generation, using Stephenson-I linkage, L_{12} should be taken as L_1 , L_{22} as L_2 , L_{31} as L_3 and L_{41} as L_4 .

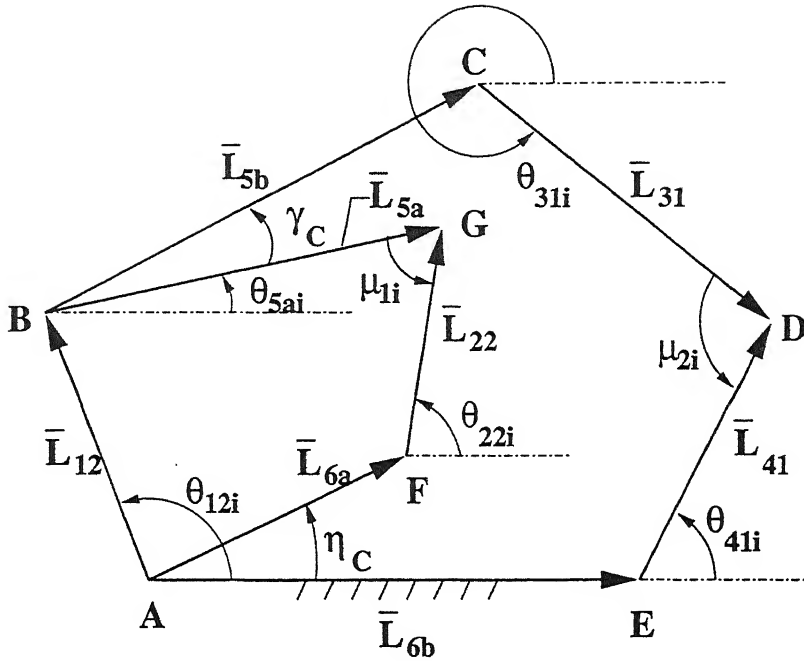


Figure 4.2: Link-vector diagram of Stephenson-I at the i^{th} design position for function generation.

and for the loop $ABGFA$, the loop closure equation is

$$\vec{L}_{12} + \vec{L}_{5a} - \vec{L}_{6a} - \vec{L}_{22} = 0. \quad (4.2)$$

Elimination of angle θ_{31} from Equation (4.1), gives

$$\begin{aligned}
 & L_{12}^2 + L_{5b}^2 + L_{41}^2 + L_{6b}^2 - L_{31}^2 + 2.L_{12}.L_{5b} \cos(\theta_{12i} - \theta_{5ai} - \gamma_c) \\
 & - 2.L_{12}.L_{6b} \cos \theta_{12i} - 2.L_{12}.L_{41} \cos(\theta_{12i} - \theta_{41i}) - 2.L_{5b}.L_{41} \cos(\theta_{5ai} + \gamma_c - \theta_{41i}) \\
 & - 2.L_{5b}.L_{6b} \cos(\theta_{5ai} + \gamma_c) + 2.L_{41}.L_{6b} \cos \theta_{41i} = 0
 \end{aligned} \quad (4.3)$$

at the i^{th} design position and elimination of θ_{22} from equation (4.2), gives

$$\begin{aligned}
 & L_{12}^2 + L_{5a}^2 + L_{6a}^2 - L_{22}^2 + 2.L_{12}.L_{5a} \cos(\theta_{12i} - \theta_{5ai}) - 2.L_{12}.L_{6a} \cos(\theta_{12i} - \eta_c) \\
 & - 2.L_{5a}.L_{6a} \cos(\theta_{5ai} - \eta_c) = 0.
 \end{aligned} \quad (4.4)$$

The values of L_{12} , L_{6b} , γ_c and η_c are assumed whereas those of θ_{12i} and θ_{41i} are determined from x and y for the N design points. The values of θ_{5ai} are assumed arbitrarily at the design points. The optimum dimensions of the linkage are those which satisfy Equations (4.3) and (4.4) at N design points in the least square sense.

Dividing Equation (4.3) by $2.L_{12}.L_{6b}$ and rearranging, the input-output relationship at the i^{th} design position is obtained as

$$\frac{L_{41}}{L_{12}} \left(\cos(\theta_{41i}) - \frac{L_{12}}{L_{6b}} \cos(\theta_{12i} - \theta_{41i}) \right) + \frac{L_{5b}}{L_{12}} \left(-\cos(\theta_{5ai} + \gamma_c) + \frac{L_{12}}{L_{6b}} c \cos \cos(\theta_{12i} - \theta_{5ai} - \gamma_c) \right) + \frac{L_{12}^2 + L_{5b}^2 + L_{41}^2 + L_{6b}^2 - L_{31}^2}{2.L_{12}.L_{6b}} - \frac{L_{5b}}{L_{12}} \cdot \frac{L_{41}}{L_{6b}} \cos(\theta_{5ai} + \gamma_c - \theta_{41i}) - \cos(\theta_{12i}) = 0,$$

or

$$D_1\mu_{1i} + D_2\mu_{2i} + D_3\mu_{3i} - D_1D_2\rho_i - \nu_i = 0 \quad (4.5)$$

where,

$$D_1 = \frac{L_{41}}{L_{12}}, D_2 = \frac{L_{5b}}{L_{12}}, D_3 = \frac{L_{12}^2 + L_{5b}^2 + L_{41}^2 + L_{6b}^2 - L_{31}^2}{2.L_{12}.L_{6b}}, \lambda = D_1D_2 = \frac{L_{41}}{L_{12}} \cdot \frac{L_{5b}}{L_{12}},$$

$$\mu_{1i} = \cos(\theta_{41i}) - \frac{L_{12}}{L_{6b}} \cos(\theta_{12i} - \theta_{41i}),$$

$$\mu_{2i} = -\cos(\theta_{5ai} + \gamma_c) + \frac{L_{12}}{L_{6b}} \cos(\theta_{12i} - \theta_{5ai} - \gamma_c), \mu_{3i} = 1,$$

$$\rho_i = \frac{L_{12}}{L_{6b}} \cos(\theta_{5ai} + \gamma_c - \theta_{41i}), \nu_i = \cos(\theta_{12i}).$$

Similarly, dividing Equation (4.4) by $2.L_{12}L_{5a}$ and rearranging one gets

$$\frac{L_{6a}}{L_{12}} \cos(\theta_{5ai} - \eta_c) + \frac{L_{6a}}{L_{5a}} \cos(\theta_{12i} - \eta_c) - \frac{L_{12}^2 + L_{5a}^2 + L_{6a}^2 - L_{22}^2}{2.L_{12}.L_{5a}}$$

$$- \cos(\theta_{12i} - \theta_{5ai}) = 0,$$

or

$$D'_1\mu'_{1i} + D'_2\mu'_{2i} + D'_3\mu'_{3i} - \nu'_i = 0 \quad (4.6)$$

where,

$$D'_1 = \frac{L_{6a}}{L_{12}}, D'_2 = \frac{L_{6a}}{L_{5a}}, D'_3 = \frac{L_{12}^2 + L_{5a}^2 + L_{6a}^2 - L_{22}^2}{2.L_{12}.L_{5a}},$$

$$\mu'_{1i} = \cos(\theta_{5ai} - \eta_c), \mu'_{2i} = \cos(\theta_{12i} - \eta_c), \mu'_{3i} = -1$$

$$v'_i = -\cos(\theta_{12i} - \theta_{5ai}) .$$

The design parameters D_1, D_2, D_3 and D'_1, D'_2, D'_3 are defined in such a way that a design parameter appears only in either Equation (4.5) or Equation (4.6). In other words, both the equations are decoupled in terms of unknown design parameters.

Equation (4.5) is a nonlinear equation while Equation (4.6) is a linear equation. Equation (4.5) is partitioned into two linear equations using the linear superposition technique, as explained in Chapter 3.

From Equation (4.5),

$$\lambda = D_1 D_2 . \quad (4.7)$$

It is defined that,

$$D_1 = p_1 + \lambda q_1, D_2 = p_2 + \lambda q_2$$

and

$$D_3 = p_3 + \lambda q_3 . \quad (4.8)$$

Equations (4.8) and (4.5) give the following two linearized equations:

$$p_1 \mu_{1i} + p_2 \mu_{2i} + p_3 \mu_{3i} - v_i = 0 \quad (4.9)$$

and

$$q_1 \mu_{1i} + q_2 \mu_{2i} + q_3 \mu_{3i} - \rho_i = 0 . \quad (4.10)$$

Equations (4.6), (4.9) and (4.10) are used to get the required unknowns, using the LSM for the N design points. Equation (4.6) gives D'_1, D'_2, D'_3 , Equation (4.9) gives p_1, p_2, p_3 and Equation (4.10) gives q_1, q_2, q_3 . The compatibility Equation (4.7) is expanded to give,

$$q_1 q_2 \lambda^2 + (p_1 q_2 + p_2 q_1 - 1) \lambda + p_1 p_2 = 0 \quad (4.11)$$

which is solved for obtaining the value(s) of λ . Once λ is known, D_1, D_2, D_3 are calculated using Equation (4.8). From D_1, D_2, D_3 and D'_1, D'_2, D'_3 all the unknown link dimensions can be determined.

A six-bar linkage has four geometric inversions. Thus, with two real values of λ there are in total, eight geometric inversions. One of these eight is the optimum solution. Further, the resulting solution generates values of θ_{5ai} which are different from the initially assumed values. These generated values can be used in place of the initial values to improve the accuracy of the generated function. Such improvement can be employed a few times. Different values of the other assumed dimensions may also be tried to increase the number of acceptable optimum linkages.

The error in the generated function at the i^{th} design point (position) is

$$e_i = (\theta_{41i})_g - (\theta_{41i})_d \quad (4.12)$$

where $(\theta_{41i})_g$ is the generated value and $(\theta_{41i})_d$ is the desired value. The efficiency of the generated approximation is tested by the average error magnitude

$$e_{avg} = \frac{1}{N} \left(\sum_{i=1}^N |e_i| \right) \quad (4.13)$$

and/or by the root-mean-square error

$$e_{rms} = \left(\frac{1}{N} \left(\sum_{i=1}^N e_i^2 \right) \right)^{\frac{1}{2}}. \quad (4.14)$$

4.3 Path Generation using Stephenson-I Linkage²

The Stephenson-I linkage at the i^{th} design position is shown in Figure 4.3. Coordinates of the design points along the path are defined by $\vec{P}_i = P_i \vec{U}_i$ in the OXY system, and \vec{P}_i 's

²In all the sections of path generation, using Stephenson-I linkage, L_{12} should be taken as L_1 , L_{22} as L_2 , L_{31} as L_3 and L_{41} as L_4 .

are specified in a design problem. $\vec{U}_i = \cos \delta_i \hat{i} + \sin \delta_i \hat{j}$ is the unit vector positioned by the angle δ_i , where \hat{i} and \hat{j} are unit vectors along X and Y respectively. The fixed link is positioned by $\vec{R}_A = R_A \vec{U}_{\alpha_A}$, $\vec{R}_E = R_E \vec{U}_{\alpha_E}$ and $\vec{R}_F = R_F \vec{U}_{\alpha_F}$. Dimensions of the linkage are defined in Figure 4.3. $\vec{\alpha}$ and β (where $\beta = \theta_{31} + \psi$) define the position of the coupler point P with respect to the coupler link. The loop-closure equation for the coupler

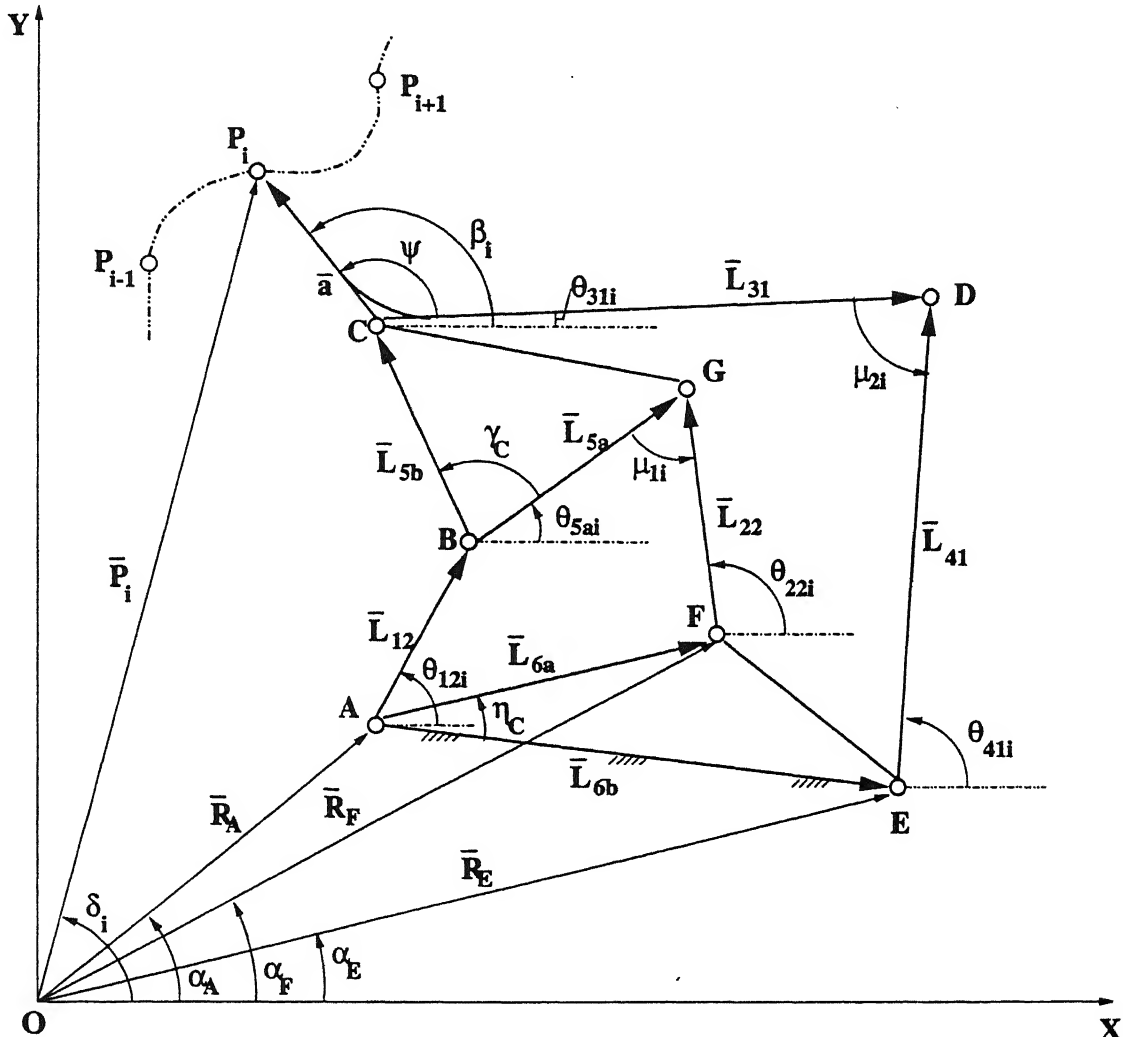


Figure 4.3: Stephenson-I, as Path Generator, at the i^{th} design position when generating a path.

point, using the loop $OABCPO$ is,

$$\vec{R}_A + \vec{L}_{12} + \vec{L}_{5b} + \vec{\alpha} - \vec{P}_i = 0. \quad (4.15)$$

The other two loop-closure equations, using $ABGFA$ and $ABCDEA$, are

$$\vec{L}_{12} + \vec{L}_{5a} - \vec{R}_{F+} \vec{R}_A - \vec{L}_{22} = 0 \quad (4.16)$$

and

$$\vec{L}_{12} + \vec{L}_{5b} + \vec{L}_{31} - \vec{R}_E + \vec{R}_A - \vec{L}_{41} = 0. \quad (4.17)$$

Elimination of angle β from Equation (4.15) at the i^{th} design position gives

$$\begin{aligned} R_A^2 + L_{12}^2 + L_{5b}^2 + P_i^2 - a^2 + 2.R_A.L_{12} \cos(\alpha_A - \theta_{12i}) + 2.R_A.L_{5b} \cos(\alpha_A - \theta_{5ai} - \gamma_c) \\ - 2.R_A.P_i \cos(\alpha_A - \delta_i) + 2.L_{12}.L_{5b} \cos(\theta_{12i} - \theta_{5ai} - \gamma_c) - 2.L_{12}.P_i \cos(\theta_{12i} - \delta_i) \\ - 2.L_{5b}.P_i \cos(\theta_{5ai} + \gamma_c - \delta_i) = 0. \end{aligned} \quad (4.18)$$

Elimination of θ_{22} from Equation (4.16) at the i^{th} design position gives

$$\begin{aligned} L_{12}^2 + L_{5a}^2 + R_F^2 + R_A^2 - L_{22}^2 + 2.L_{12}.L_{5a} \cos(\theta_{12i} - \theta_{5ai}) - 2.L_{12}.R_F \cos(\theta_{12i} - \alpha_F) \\ + 2.L_{12}.R_A \cos(\theta_{12i} - \alpha_A) - 2.L_{5a}.R_F \cos(\theta_{5ai} - \alpha_F) + 2.L_{5a}.R_A \cos(\theta_{5ai} - \alpha_A) \\ - 2.R_F.R_A \cos(\alpha_F - \alpha_A) = 0. \end{aligned} \quad (4.19)$$

Similarly, elimination of θ_{41} from Equation (4.17) gives

$$\begin{aligned} L_{12}^2 + L_{5b}^2 + L_{31}^2 + R_E^2 + R_A^2 - L_{41}^2 + 2.L_{12}.L_{5b} \cos(\theta_{12i} - \theta_{5ai} - \gamma_c) \\ + 2.L_{12}.L_{31} \cos(\theta_{12i} - \theta_{31i}) - 2.L_{12}.R_E \cos(\theta_{12i} - \alpha_E) + 2.L_{12}.R_A \cos(\theta_{12i} - \alpha_A) \\ + 2.L_{5b}.L_{31} \cos(\theta_{5ai} + \gamma_c - \theta_{31i}) - 2.L_{5b}.R_E \cos(\theta_{5ai} + \gamma - \alpha_E) + 2.L_{5b}.R_A \cos(\theta_{5ai} + \gamma - \alpha_A) \\ - 2.L_{31}.R_E \cos(\theta_{31i} - \alpha_E) + 2.L_{31}.R_A \cos(\theta_{31i} - \alpha_A) - 2.R_E.R_A \cos(\alpha_E - \alpha_A) = 0. \end{aligned} \quad (4.20)$$

Equations (4.18), (4.19), and (4.20) are the design equations that must be satisfied at the N design points. At each design point values of \vec{P}_i , θ_{21i} and θ_{5ai} are specified. The values of θ_{31i} to be used in Equation (4.20) are obtained after solving Equation (4.18) and using the separated x and y components of the loop-closure Equation (4.15). Thus,

$$\tan(\theta_{31i} + \psi) = \frac{P_i \sin(\delta_i) - R_A \sin(\alpha_A) - L_{12} \sin(\theta_{12i}) - L_{5b} \sin(\theta_{5ai} + \gamma_c)}{P_i \cos(\delta_i) - R_A \cos(\alpha_A) - L_{12} \cos(\theta_{12i}) - L_{5b} \cos(\theta_{5ai} + \gamma_c)} \quad (4.21)$$

The values of L_{12} , α_A , α_E , α_F , ψ and γ_c are initially assumed. The remaining dimensions L_{22} , L_{31} , L_{41} , L_{5a} , L_{5b} , L_{6a} , L_{6b} , R_A , R_E and R_F are obtained by applying the LSM.

Equation (4.18) is rearranged as

$$D_1\mu_{1i} + D_2\mu_{2i} + D_3\mu_{3i} - D_1D_2\rho_i - \nu_i = 0 \quad (4.22)$$

where,

$$\begin{aligned} D_1 &= R_A, D_2 = L_{5b}, D_3 = R_A^2 + L_{12}^2 + L_{5b}^2 - a^2, \lambda = D_1D_2 = R_A \cdot L_{5b}, \\ \mu_{1i} &= 2 \cdot L_{12} \cos(\theta_{12i} - \alpha_A) - 2 \cdot P_i \cos(\alpha_A - \delta_i), \\ \mu_{2i} &= 2 \cdot L_{12} \cos(\theta_{12i} - \theta_{5ai} - \gamma_c) - 2 \cdot P_i \cos(\theta_{5ai} + \gamma_c - \delta_i), \mu_{3i} = 1, \\ \rho_i &= -2 \cos(\alpha_A - \theta_{5ai} - \gamma_c), \nu_i = 2 \cdot L_{12} \cdot P_i \cos(\theta_{12i} - \delta_i) - P_i^2. \end{aligned}$$

Equation (4.19) is rearranged as

$$D'_1\mu'_{1i} + D'_2\mu'_{2i} + D'_3\mu'_{3i} - D'_1D'_2\rho'_i - \nu'_i = 0 \quad (4.23)$$

where,

$$\begin{aligned} D'_1 &= L_{5a}, D'_2 = R_F, D'_3 = L_{12}^2 + L_{5a}^2 + R_F^2 + R_A^2 - L_{22}^2, \lambda' = D'_1D'_2 = L_{5a} \cdot R_A, \\ \mu'_{1i} &= 2 \cdot L_{12} \cos(\theta_{12i} - \theta_{5ai}) + 2 \cdot R_A \cos(\theta_{5ai} - \alpha_A), \\ \mu'_{2i} &= 2 \cdot L_{12} \cos(\theta_{12i} - \alpha_F) - 2 \cdot R_A \cos(\alpha_F - \alpha_A), \mu'_{3i} = 1, \\ \rho'_i &= 2 \cos(\theta_{5ai} - \alpha_F), \nu'_i = -2 \cdot L_{12} \cdot R_A \cos(\theta_{12i} - \alpha_A). \end{aligned}$$

Similarly, Equation (4.20) gives

$$D_1''\mu_{1i}'' + D_2''\mu_{2i}'' + D_3''\mu_{3i}'' - D_1''D_2''\rho_i'' - \nu_i'' = 0 \quad (4.24)$$

where,

$$\begin{aligned} D_1'' &= L_{31}, D_2'' = R_E, D_3'' = L_{12}^2 + L_{5b}^2 + L_{31}^2 + R_E^2 + R_A^2 - L_{41}^2, \lambda'' = D_1''D_2'' = L_{31} \cdot R_E, \\ \mu_{1i}'' &= 2 \cdot L_{12} \cos(\theta_{12i} - \theta_{31i}) + 2 \cdot L_{5b} \cos(\theta_{5ai} + \gamma_c - \theta_{31i}) + 2 \cdot R_A \cos(\theta_{31i} - \alpha_A), \\ \mu_{2i}'' &= -2 \cdot L_{12} \cos(\theta_{12i} - \alpha_E) - 2 \cdot L_{5b} \cos(\theta_{5ai} + \gamma_c - \alpha_E) - 2 \cdot R_A \cos(\alpha_E - \alpha_A), \mu_{3i}'' = 1, \\ \rho_i'' &= 2 \cos(\theta_{31i} - \alpha_E), \end{aligned}$$

$$\nu_i'' = -2 \cdot L_{12} \cdot L_{5b} \cos(\theta_{12i} - \theta_{5ai} - \gamma) - 2 \cdot L_{12} \cdot R_A \cos(\theta_{12i} - \alpha_A) - 2 \cdot L_{5b} \cdot R_A \cos(\theta_{5ai} + \gamma_c - \alpha_A).$$

Equations (4.22), (4.23) and (4.24) have nonlinearity coefficients as $\lambda = D_1 D_2$, $\lambda' = D_1' D_2'$ and $\lambda'' = D_1'' D_2''$, respectively. These are linearized by the linear superposition technique as had been explained in the previous section for the function generation problem.

The maximum number of solutions possible in the path generation problem is $2 \times 2 \times 2 \times 4 = 32$. Out of these one or more solutions will satisfy the problem up to the desired accuracy. The errors in the approximation are defined as follows to check the efficiency of the method. The average error is given by

$$e_{avg} = \frac{1}{2N} \left(\sum_{i=1}^N (|x_g - x_d| + |y_g - y_d|)_i \right) \quad (4.25)$$

and the root-mean-square error

$$e_{rms} = \left[\frac{1}{2N} \sum_{i=1}^N \left\{ (x_g - x_d)_i^2 + (y_g - y_d)_i^2 \right\} \right]^{\frac{1}{2}}. \quad (4.26)$$

4.4 Motion Generation using Watt-II Linkage³

Figure 4.4 shows a Watt-II linkage with link DE as the carrier link, coupler point P as the generator of the path. The rigid body, shown in the Figure 4.4, is positioned by positioning the body-line PQ . When guiding a rigid body, the angular dimension ϵ controls the position of the rigid body-line with respect to the link-line of the generator link. If ϵ is taken as an unknown dimension, it increases the number of compatibility equations to be satisfied, hence it is preferable to specify ϵ . In the following developments, the value of ϵ is taken to be known and is taken to be positive⁴. At N design positions the value of \vec{P}_i (where $\vec{P}_i = P_i \vec{U}_i$ in the OXY system, as defined in the previous section. $\vec{U}_i = \cos \delta_i \hat{i} + \sin \delta_i \hat{j}$ is the unit vector positioned by the angle δ_i .) and ξ_i (anexit

gle made by \vec{PQ} at the i^{th} design position) are specified as required by the design. The three loop-closure equations for the loops $OAFPO$, $OBCGAO$ and $FGDEF$, respectively, are

$$\vec{R}_A + \vec{L}_{6b} + \vec{\alpha} - \vec{P}_i = 0 \quad (4.27)$$

$$\vec{R}_B + \vec{L}_{21} + \vec{L}_{5a} - \vec{L}_{6a} - \vec{R}_A = 0 \quad (4.28)$$

and

$$\vec{L}_{6b} - \vec{L}_{6a} + \vec{L}_{5b} - \vec{L}_{5a} + \vec{L}_{31} + \vec{L}_{41} = 0. \quad (4.29)$$

It is seen from the Figure 4.4, that

$$\theta_{41i} = \xi_i - \epsilon \quad (4.30)$$

and

$$\beta_i = \theta_{41i} + (180^\circ - \psi)$$

³In all the sections of motion generation, using Watt-II linkage, L_{11} should be taken as L_1 , L_{21} as L_2 , L_{31} as L_3 and L_{41} as L_4 .

⁴i.e., the value of ϵ is specified between 0° and 360° .

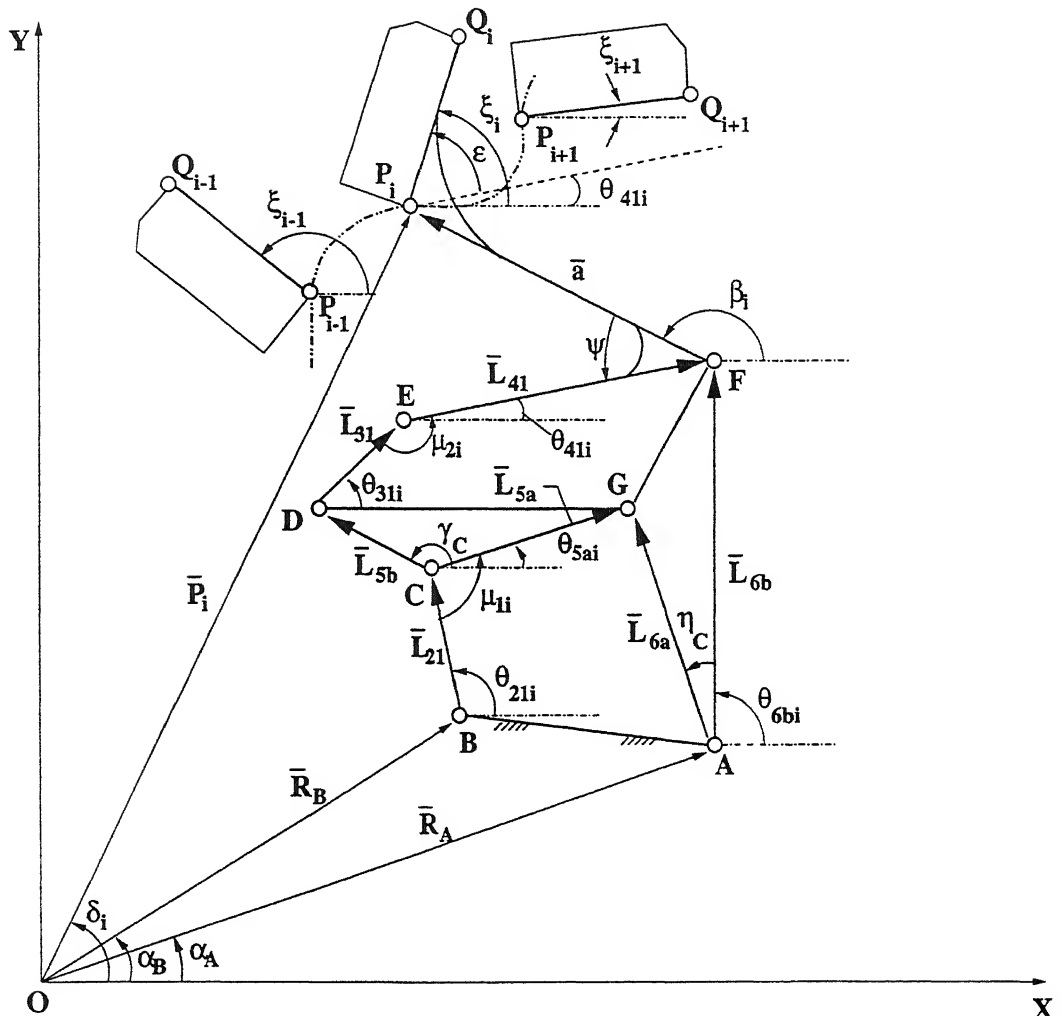


Figure 4.4: Watt-II, as Motion Generator, at the i^{th} design position generating rigid-body motion.

or

$$\beta_i = \xi_i - \epsilon + (180^\circ - \psi) . \quad (4.31)$$

The values of L_{6a} , α_A , α_B , γ_c , η_c and ϵ are specified. The values of θ_{5ai} are assumed for each design position in accordance with P_i and ξ_i . The remaining unknown dimensions are found from the synthesis.

Elimination of angle θ_{6b} from Equation (4.27) at the i^{th} design position gives

$$R_A^2 + a^2 + P_i^2 - L_{6b}^2 + 2.R_A.a \cos(\alpha_A - \beta_i) - 2.R_A.P_i \cos(\alpha_A - \delta_i) - 2.a.P_i \cos(\beta_i - \delta_i) = 0 . \quad (4.32)$$

Elimination of θ_{21} from Equation (4.28) at the i^{th} design position gives. $R_{_}$

$$\begin{aligned} R_B^2 + L_{5a}^2 + L_{6a}^2 + R_A^2 - L_{21}^2 + 2.R_B.L_{5a} \cos(\alpha_B - \theta_{5ai}) - 2.R_B.L_{6a} \cos(\alpha_B - \theta_{6ai}) \\ - 2.R_B.R_A \cos(\alpha_B - \alpha_A) - 2.L_{5a}.L_{6a} \cos(\theta_{5ai} - \theta_{6ai}) - 2.L_{5a}.R_A \cos(\theta_{5ai} - \alpha_A) \\ + 2.L_{6a}.R_A \cos(\theta_{6ai} - \alpha_A) = 0 . \end{aligned} \quad (4.33)$$

Similarly, elimination of θ_{31} from Equation (4.29) gives

$$\begin{aligned} L_{6b}^2 + L_{6a}^2 + L_{5b}^2 + L_{5a}^2 + L_{41}^2 - L_{31}^2 - 2.L_{6b}.L_{6a} \cos(\eta_c) + 2.L_{6b}.L_{5b} \cos(\theta_{6ai} - \eta_c - \theta_{5ai} - \gamma_c) \\ 2.L_{6b}.L_{5a} \cos(\theta_{6ai} - \eta - \theta_{5ai}) + 2.L_{6b}.L_{41} \cos(\theta_{6ai} - \eta_c - \theta_{41i}) - 2.L_{6a}.L_{5b} \cos(\theta_{6ai} - \theta_{5ai} - \gamma_c) \\ + 2.L_{6a}.L_{5a} \cos(\theta_{6ai} - \theta_{5ai}) - 2.L_{6a}.L_{41} \cos(\theta_{6ai} - \theta_{41i}) - 2.L_{5b}.L_{5a} \cos(\gamma_c) \\ + 2.L_{5b}.L_{41} \cos(\theta_{5ai} + \gamma_c - \theta_{41}) - 2.L_{5a}.L_{41} \cos(\theta_{5ai} - \theta_{41i}) = 0 . \end{aligned} \quad (4.34)$$

The values of θ_{6ai} to be used in Equations (4.33) and (4.34) are obtained after solving Equation (4.32) and then using the separated x and y components of Equation (4.27).

Thus,

$$\tan(\theta_{6ai} - \eta_c) = \frac{P_i \sin(\delta_i) - R_A \sin(\alpha_A) - a \sin(\beta_i)}{P_i \cos(\delta_i) - R_A \cos(\alpha_A) - a \cos(\beta_i)}. \quad (4.35)$$

Equation (4.32) is rearranged as

$$D_1\mu_{1i} + D_2\mu_{2i} + D_3\mu_{3i} - D_1D_2\rho_i - \nu_i = 0 \quad (4.36)$$

where,

$$\begin{aligned} D_1 &= R_A, D_2 = a, D_3 = R_A^2 + a^2 - L_{6b}^2, \lambda = D_1D_2 = R_A \cdot a, \\ \mu_{1i} &= -2.P_i \cos(\alpha_A - \delta_i), \\ \mu_{2i} &= -2.P_i \cos(\beta_i - \delta_i), \mu_{3i} = 1, \\ \rho_i &= -2 \cos(\alpha_A - \beta_i), \nu_i = -P_i^2. \end{aligned}$$

Equation (4.33) is rearranged as

$$D'_1\mu'_{1i} + D'_2\mu'_{2i} + D'_3\mu'_{3i} - D'_1D'_2\rho'_i - \nu'_i = 0 \quad (4.37)$$

where,

$$\begin{aligned} D'_1 &= R_B, D'_2 = L_{5a}, D'_3 = R_B^2 + L_{5a}^2 + L_{6a}^2 + R_A^2 - L_{21}^2, \lambda' = D'_1D'_2 = R_b \cdot L_{5a}, \\ \mu'_{1i} &= -2.R_A \cos(\alpha_A - \alpha_B) + 2.L_{6a} \cos(\alpha_A - \theta_{6ai}), \\ \mu'_{2i} &= -2.L_{6a} \cos(\theta_{5ai} - \theta_{6ai}) - 2.R_A \cos(\theta_{5ai} - \alpha_A), \mu'_{3i} = 1, \\ \rho'_i &= -2 \cos(\alpha_B - \theta_{5ai}), \nu'_i = -2.L_{6a} \cdot R_A \cos(\theta_{6ai} - \alpha_A). \end{aligned}$$

Similarly, Equation (4.34) gives

$$D''_1\mu''_{1i} + D''_2\mu''_{2i} + D''_3\mu''_{3i} - D''_1D''_2\rho''_i - \nu''_i = 0 \quad (4.38)$$

where,

$$\begin{aligned} D''_1 &= L_{5b}, D''_2 = L_{41}, D''_3 = L_{6b}^2 + L_{6a}^2 + L_{5b}^2 + L_{5a}^2 + L_{41}^2 - L_{31}^2, \lambda'' = D''_1D''_2 = L_{5b} \cdot L_{41}, \\ \mu''_{1i} &= 2.L_{6b} \cos(\theta_{6ai} - \eta_c - \theta_{5ai} - \gamma_c) - 2.L_{6a} \cos(\theta_{6ai} - \theta_{5ai} - \gamma_c) - 2.L_{5a} \cos(\gamma_c), \\ \mu''_{2i} &= 2.L_{6b} \cos(\theta_{6ai} - \eta_c - \theta_{41i}) - 2.L_{6a} \cos(\theta_{6ai} - \theta_{41i}) - 2.L_{5a} \cos(\theta_{5ai} - \theta_{41i}), \mu''_{3i} = 1, \end{aligned}$$

$$\rho_i'' = -2 \cos(\theta_{5ai} + \gamma_c - \theta_{41i}),$$

$$\nu_i'' = -2.L_{6b}.L_{6a} \cos(\eta_c) - 2.L_{6b}.L_{5a} \cos(\theta_{6ai} - \eta_c - \theta_{5ai}) + 2.L_{6a}.L_{5a} \cos(\theta_{6ai} - \theta_{5ai}).$$

Equations (4.36), (4.37) and (4.38) have nonlinearity coefficients as $\lambda = D_1 D_2$, $\lambda' = D'_1 D'_2$ and $\lambda'' = D''_1 D''_2$, respectively. These are linearized by the linear superposition technique.

All these equations give maximum $2 \times 2 \times 2 = 8$ sets of dimensions, therefore $4 \times 8 = 32$ linkages are defined by geometric inversions, out of which one or more are the optimum solutions. The angular error in the generated motion at the i^{th} design position is

$$e_i = (\theta_{41i} + \epsilon)_g - (\xi_i)_d \quad (4.39)$$

where $(\theta_{41i})_g$ is the generated value. The average error magnitude is given by

$$e_{avg} = \frac{1}{N} \left(\sum_{i=1}^N |e_i| \right) \quad (4.40)$$

and the root-mean-square error as

$$e_{rms} = \left(\frac{1}{N} \left(\sum_{i=1}^N e_i^2 \right) \right)^{\frac{1}{2}}. \quad (4.41)$$

The errors in the generated path are defined by Equations (4.25) and (4.26).

4.5 Numerical Examples

Computer programs in C++ (Borland 4.5) have been developed which perform the optimum synthesis of Stephenson-I for function generation and path generation problems and Watt-II for motion generation problems. This section illustrates some examples giving the results generated by those programs.

Example 1: Stephenson-I linkage is synthesized to generate the symmetric function

$$y = x^2, \quad -1 \leq x \leq +1.$$

within the intervals⁵ $\Delta\theta_{12} = 90^\circ$ and $\Delta\theta_{41} = 60^\circ$. Nineteen uniformly distributed design positions are used. Values of x and y are given in Table 4.1, where the subscript d designates the "desired value" while g designates the "generated value". The specified dimensions (Figure 4.2) are $L_{12} = 20$ cm, $L_{6b} = 40$ cm, $\eta_c = -142^\circ$, $\gamma_c = -154^\circ$, $\theta_{12}^1 = 50^\circ$ and $\theta_{41}^1 = 10^\circ$. After solving the design equations, two distinct values of λ are obtained as -139.606 and -0.875 . The optimum linkage⁶ was obtained using $\lambda = -0.875$. The average error is $e_{avg} = 0.622^\circ$ and the root-mean-square error is $e_{rms} = 0.768^\circ$. Table 4.2⁷ gives the displacements of the linkage and the error in the generated function along with the specified values of θ_{12i} , θ_{5ai} and θ_{41i} . The dimensions of the linkage and the transmission angles μ_1 and μ_2 are also given. The values of all the link-lengths have been made positive with the corresponding changes in their respective angular displacements.

Table 4.1 also gives the generated values of y at the design positions. Table 4.3 gives the values of the displacements obtained when the values of θ_{5ai} generated in the first optimization process ($(\theta_{5ai})_g$ in Table 4.1) are used as the input for a improved solution. It is seen that the solution obtained does not prove to be a better solution. Hence, the linkage obtained in the first optimization process is taken as the optimum solution linkage.

From Table 4.2, it is seen that the error in the generated function has a maximum value of -1.794° . In reference [7] (Table 10.3, p. 314), the maximum value of error generated by a planar four-bar linkage, for the same function and same input-output range of motions with five precision points, is given as 2.34° . Though the improvement obtained by the six-bar linkage is not much but it can be hoped that a better solution can be obtained with

⁵Relationship between x and θ_{12} , and y and θ_{41} is given at the end of *Example 1*.

⁶The linkage obtained using $\lambda = -139.606$ gave $e_{avg} = 24.870^\circ$ and $e_{rms} = 28.315^\circ$.

⁷All the angles, in the given Tables, are in degrees. All the numerical values are given up to the third decimal place.

a different set of initial data.

A linear relationship is assumed between Δx and $\Delta\theta_{12}$, given by

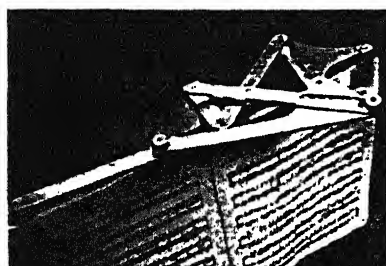
$$\theta_{12}^i - \theta_{12}^1 = (x^i - x^1) \frac{\Delta\theta_{12}}{\Delta x}.$$

Similarly, a linear relationship is given between Δy and $\Delta\theta_{41}$ is given by

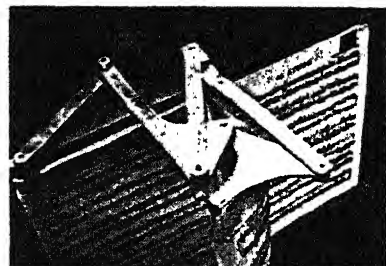
$$\theta_{41}^i - \theta_{41}^1 = (y^i - y^1) \frac{\Delta\theta_{41}}{\Delta y}.$$

the pages of a music book automatically (reference [5], Problem 1.42, p. 67). The linkage is shown in Figure 4.6. To the upper right-hand corner of each page a magnetic strip is attached. The linkage is to have a crank input (possibly actuated by a foot switch).

Eighteen design positions are used whose co-ordinates are given in Table 4.6. The specified dimensions⁸ (Figure 4.3) are $L_{12} = 60$ cm $\alpha_A = 180^\circ$, $\alpha_E = 0^\circ$, $\alpha_F = -103^\circ$, $\gamma_c = -20^\circ$ and $\psi = 60^\circ$. Only 16 geometric inversions out of 32 had mobility within the zone of motion. The linkage with the best performance is shown in Figure 4.7. The values of errors generated are $e_{avg} = 2.746$ cm and $e_{rms} = 2.382$ cm. The minimum values of the transmission angles are $\mu_{1min} = 25.011^\circ$ and $\mu_{2min} = 32.436^\circ$. The errors in the generated coordinates are given in Table 4.6. Table 4.7 gives the dimensions and the displacements generated by this linkage.



(a)



(b)

Figure 4.6: Page turning linkage.

Example 4: Watt-II linkage is synthesized to guide the door-board of a vehicle garage (reference [6], Problem 6.3-2, pp.246-7). The linkage is designed so as to have the motion of the door without touching the vehicle that is parked inside the garage, :

⁸The dimensions of the linkage correspond to a scaled model and not to the actual linka

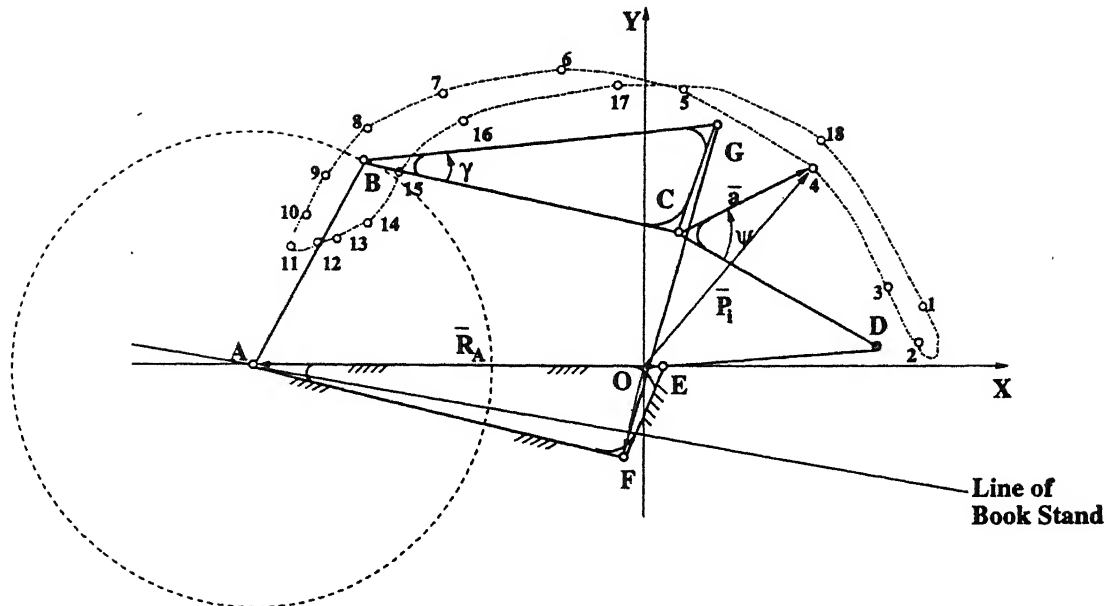


Figure 4.7: Stephenson-I linkage optimized in Example 3 to generate path for the page turning linkage.

Figure 4.8. Both the desired (marked by o) and the generated curves traced by the end of the door-board are indicated in Figure 4.8. Sixteen design positions of the rigid-body (i.e., the door-board) are taken as given in Table 4.8. The specified dimensions⁹ (Figure 4.4) are $L_{6a} = 15$ cm, $\alpha_A = 0^\circ$, $\alpha_B = 44^\circ$, $\gamma_c = -90^\circ$, $\eta_c = 0^\circ$, $\psi = 9^\circ$ and $\epsilon = 351^\circ$. Only four geometric inversions out of 32 had mobility within the specified zone of motion. The optimum solution, shown in Figure 4.9, guides the door-board with *angular* $e_{avg} = 1.713^\circ$, *angular* $e_{rms} = 2.110^\circ$, *linear* $e_{avg} = 3.075$ cm and *linear* $e_{rms} = 2.995$ cm. Table 4.9 gives the values of the specified θ_{5ai} along with the generated displacements.

It should be noted that the value of link-length L_{5b} is very small as compared to other link-lengths, suggesting that one can make the hinge C of second order where links 2, 3 and 5 are all connected. Table 4.10 and Table 4.11 give the values of the displacements of all the links under such a situation. It may be mentioned that the door-board, taken as the coupler of a four-bar linkage could never achieve this motion. It would have required a much larger overhead space in order to avoid the vehicle body.

⁹The dimensions of the linkage correspond to a scaled model and not to the actual linkage.

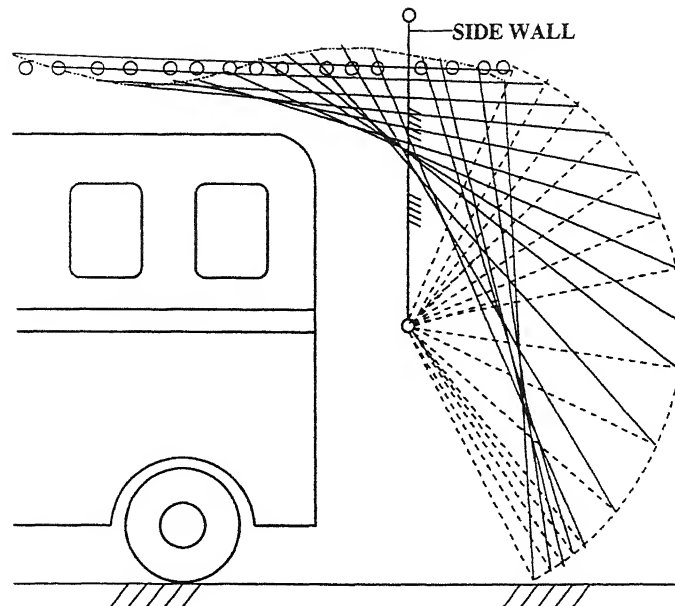


Figure 4.8: The available space inside the garage is determined by the envelope of the straight lines, representing the garage-door at various positions.

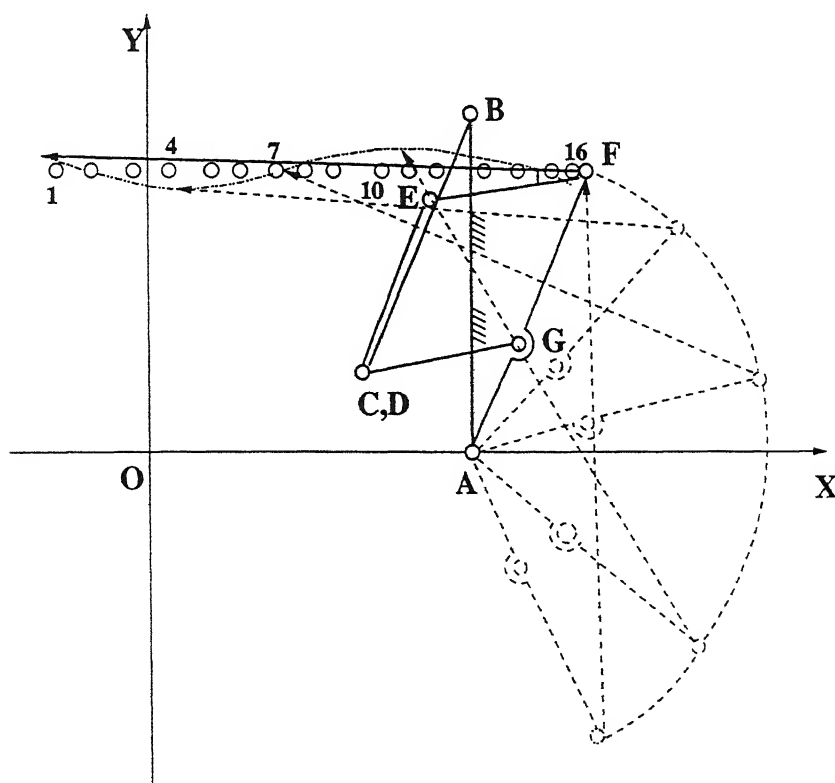


Figure 4.9: Watt-II linkage optimized in Example 4 to guide the garage-door.

4.6 Conclusions

The Least Square error Method and the Linear Superposition Technique provide a powerful and efficient synthesis method. The number of unknown dimensions can be increased in each case of synthesis. This in turn increases the complexity of the equations leading to more than one compatibility equations. For the solution of more than one compatibility equations, *Sylvester's Dialytic Method of Elimination*³ has to be used [11-13]. The number of solutions obtained also increases with the increase in the number of unknowns. Hence to keep the mathematics simple and the number of solutions manageable, the synthesis with higher number of unknowns has not been pursued in the present work.

Different initial values of the specified variables result in different linkages, thus permitting infinite number of solutions. During the calculation, conditions may arise, such that any parameter gets a non-real value. In such conditions, the synthesis should be stopped at that place and restarted with changed initial values. However, this choice of initial values is very critical for obtaining a good solution. A number of trials is often necessary to arrive at an acceptable solution which can then be easily refined to obtain a better solution. This shortcoming becomes more pronounced, when a crank is needed as the input link (continuous rotation in one direction). The difficulty can be well understood by taking the case of function generation. Referring to Figure 4.1, suppose link 1 of the Stephenson-I is to be a crank for certain oscillation of the rocker link 4. The problem becomes complicated because the loop $ABGF$, is now a four-bar crank rocker, hence the rocker, i.e., link 2 can not cross the line of frame, i.e., the line made by AF . Moreover the loop $ABGF$ should satisfy the Grashofian condition, with link 1 as the smallest link. The initial specifications of L_{6b} , L_{5b} , θ_{5a} , γ_c and η_c should be such so as to satisfy the above conditions with minimum error in the generated function. The complexity further increases in the cases of path generation and motion generation, where there are three loop closure equations to be satisfied, leading many times to abandon the initial set of the specified dimensions and the

³For details see Böcher, M., *Introduction to Higher Algebra*, Macmillan, 1949, pp. 195-202.

angular values.

Apart from the values of the error in the approximations, transmission angles as well as the maximum link-length ratio (i.e., compactness of the linkage) can also be taken as criteria for selection of the optimum

The Least Square Error Method for loop-by-loop synthesis of planar six-bar linkages for function generation, path generation and motion generation, using the linear superposition technique leads to efficient linkage designs without involving iterative solutions. The process can be repeated by reusing the generated value to improve the efficiency.

Table 4.1 Desired displacements for the function ($y = x^2$, $-1 \leq x \leq +1$) for which Stephenson-I linkage is optimized in Example 1.

i	x_i	$(y_i)_d$	$(y_i)_g$	$(y_i)_g - (y_i)_d$
1	-1.000	1.000	1.005	0.005
2	-0.889	0.790	0.792	0.002
3	-0.778	0.605	0.609	0.004
4	-0.667	0.444	0.448	0.004
5	-0.556	0.309	0.309	0.001
6	-0.444	0.198	0.193	-0.005
7	-0.333	0.111	0.100	-0.011
8	-0.222	0.049	0.035	-0.015
9	-0.111	0.012	-0.001	-0.013
10	0.000	0.000	-0.006	-0.006
11	0.111	0.012	0.016	0.004
12	0.222	0.049	0.062	0.013
13	0.333	0.111	0.128	0.017
14	0.444	0.198	0.212	0.015
15	0.556	0.309	0.314	0.006
16	0.667	0.444	0.437	-0.008
17	0.778	0.605	0.584	-0.021
18	0.889	0.790	0.770	-0.020
19	1.000	1.000	1.030	0.030

Table 4.2 Desired and generated displacements for the Stephenson-I linkage in Example 1 for function generation. $\Delta\theta_{12} = 90^\circ$, $\Delta\theta_{41} = 60^\circ$.

i	θ_{12i}	$(\theta_{5ai})_d$	$(\theta_{5ai})_g$	$(\theta_{22i})_g$	$(\theta_{31i})_g$	$(\theta_{41i})_d$	$(\theta_{41i})_g$	e_i	μ_{1i}	μ_{2i}
1	50.000	-170.426	-170.510	55.486	-75.940	10.000	9.724	-0.276	45.996	85.664
2	55.000	-169.012	-169.056	58.998	-73.743	22.593	22.451	-0.142	48.054	83.806
3	60.000	-168.013	-168.076	62.623	-72.146	33.704	33.488	-0.216	50.699	74.366
4	65.000	-167.452	-167.514	66.338	-70.902	43.333	43.110	-0.223	53.852	65.988
5	70.000	-167.302	-167.315	70.124	-69.821	51.481	51.432	-0.049	57.439	58.747
6	75.000	-167.502	-167.434	73.962	-68.738	58.148	58.435	0.287	61.396	52.827
7	80.000	-167.983	-167.836	77.834	-67.501	63.333	63.991	0.658	65.670	48.508
8	85.000	-168.682	-168.496	81.723	-65.971	67.037	67.909	0.872	70.219	46.120
9	90.000	-169.560	-169.397	85.614	-64.047	69.259	70.034	0.775	75.011	45.919
10	95.000	-170.610	-170.534	89.493	-61.689	70.000	70.356	0.356	80.027	47.954
11	100.000	-171.857	-171.909	93.344	-58.922	69.259	69.027	-0.232	85.253	52.051
12	105.000	-173.353	-173.536	97.150	-55.808	67.037	66.278	-0.759	89.314	57.914
13	110.000	-175.173	-175.438	100.894	-52.414	63.333	62.318	-1.015	83.669	65.268
14	115.000	-177.406	-177.653	104.552	-48.795	58.148	57.269	-0.879	77.795	73.936
15	120.000	179.863	179.761	108.097	-44.991	51.481	51.141	-0.340	71.663	83.868
16	125.000	176.564	176.716	111.492	-41.030	43.333	43.811	0.478	65.224	84.841
17	130.000	172.672	173.080	114.682	-36.938	33.704	34.950	1.246	58.398	71.888
18	135.000	168.244	168.635	117.585	-32.779	22.593	23.806	1.213	51.050	56.585
19	140.000	163.506	162.995	120.063	-28.874	10.000	8.206	-1.794	42.933	37.080

$$e_{avg} = 0.622^\circ \quad e_{rms} = 0.768^\circ$$

$$L_{12} = 20.000 \text{ cm} \quad L_{22} = 26.175 \text{ cm} \quad L_{31} = 35.000 \text{ cm} \quad L_{41} = 10.000 \text{ cm}$$

$$L_{5a} = 7.765 \text{ cm} \quad L_{5b} = 35.000 \text{ cm} \quad L_{6a} = 12.226 \text{ cm} \quad L_{6b} = 40.000 \text{ cm}$$

$$\eta_c = -142.000^\circ \quad \gamma_c = -154.000^\circ$$

Table 4.3 Generated displacements for the Stephenson-I linkage in Example when $(\theta_{5ai})_g$ of Table 4.1 are used as input values.

i	θ_{12i}	$(\theta_{5ai})_d$	$(\theta_{5ai})_g$	$(\theta_{22i})_g$	$(\theta_{31i})_g$	$(\theta_{41i})_d$	$(\theta_{41i})_g$	e_i	μ_{1i}	μ_{2i}	
1	50.000	-170.510	-170.510	55.485	-75.948	10.000	9.719	-0.281	45.996	85.667	
2	55.000	-169.056	-169.056	58.998	-73.751	22.593	22.451	-0.142	48.054	83.798	
3	60.000	-168.076	-168.076	62.622	-72.154	33.704	33.493	-0.211	50.698	74.353	
4	65.000	-167.514	-167.514	66.338	-70.910	43.333	43.119	-0.214	53.852	65.971	
5	70.000	-167.315	-167.315	70.124	-69.830	51.481	51.444	-0.037	57.439	58.726	
6	75.000	-167.434	-167.434	73.962	-68.748	58.148	58.451	0.303	61.396	52.802	
7	80.000	-167.836	-167.836	77.834	-67.511	63.333	64.010	0.677	65.670	48.480	
8	85.000	-168.496	-168.496	81.723	-65.981	67.037	67.929	0.892	70.219	46.090	
9	90.000	-169.397	-169.397	85.615	-64.057	69.259	70.054	0.795	75.012	45.889	
10	95.000	-170.534	-170.534	89.493	-61.699	70.000	70.374	0.374	80.027	47.926	
11	100.000	-171.909	-171.909	93.344	-58.932	69.259	69.042	-0.217	85.253	52.026	
12	105.000	-173.536	-173.536	97.151	-55.817	67.037	66.289	-0.748	89.313	57.894	
13	110.000	-175.438	-175.437	100.895	-52.422	63.333	62.325	-1.008	83.668	65.253	
14	115.000	-177.653	-177.653	104.553	-48.803	58.148	57.271	-0.877	77.794	73.925	
15	120.000	179.761	179.761	108.099	-45.000	51.481	51.138	-0.343	71.662	83.862	
16	125.000	176.716	176.716	111.493	-41.039	43.333	43.802	0.469	65.223	84.841	
17	130.000	173.080	173.080	114.683	-36.947	33.704	34.934	1.230	58.396	71.881	
18	135.000	168.635	168.635	117.587	-32.789	22.593	23.781	1.188	51.048	56.570	
19	140.000	162.995	162.995	120.064	-28.889	10.000	8.158	-1.842	42.930	37.048	
$e_{avg} = 0.624^\circ$		$e_{rms} = 0.773^\circ$									
$L_{12} = 20.000 \text{ cm}$		$L_{22} = 26.174 \text{ cm}$		$L_{31} = 35.001 \text{ cm}$		$L_{41} = 10.000 \text{ cm}$					
$L_{5a} = 7.764 \text{ cm}$		$L_{5b} = 35.001 \text{ cm}$		$L_{6a} = 12.225 \text{ cm}$		$L_{6b} = 40.000 \text{ cm}$					
$\eta_c = -142.000^\circ$		$\gamma_c = -154.000^\circ$									

Table 4.4 Desired and generated displacements for the Stephenson-I linkage in Example 2 for an output oscillation angle of more than 180° .

i	θ_{12i}	$(\theta_{5ai})_d$	$(\theta_{5ai})_g$	$(\theta_{22i})_g$	$(\theta_{31i})_g$	$(\theta_{41i})_d$	$(\theta_{41i})_g$	e_i	μ_{1i}	μ_{2i}	
1	0.000	45.000	43.356	55.950	-66.338	-5.000	-11.170	-6.170	12.594	55.168	
2	30.000	15.000	15.525	32.490	-87.674	-60.000	-50.346	9.654	16.965	37.328	
3	60.000	16.000	15.715	56.777	-69.493	12.000	8.597	-3.403	41.063	78.090	
4	90.000	18.000	17.413	82.407	-57.903	55.000	53.041	-1.959	64.994	69.056	
5	120.000	20.000	20.053	107.104	-48.890	90.000	90.374	0.374	87.051	40.736	
6	150.000	24.000	24.236	129.328	-40.525	118.000	120.113	2.113	74.908	19.362	
7	180.000	31.000	31.214	146.629	-30.358	130.000	133.307	3.307	64.586	16.335	
8	-150.000	42.000	42.154	156.341	-20.849	140.000	134.205	-5.795	65.814	24.947	
9	-120.000	56.000	56.210	158.169	-14.847	130.000	130.580	0.580	78.041	34.573	
10	-90.000	71.000	70.474	153.347	-12.233	118.000	120.585	2.585	82.874	47.182	
11	-60.000	82.000	80.676	140.984	-14.929	100.000	102.604	2.604	60.308	62.466	
12	-30.000	75.000	78.220	114.402	-28.327	70.000	70.350	0.350	36.182	81.323	
$e_{avg} = 3.241^\circ$		$e_{rms} = 4.181^\circ$									
$L_{12} = 4.500 \text{ cm}$		$L_{22} = 5.600 \text{ cm}$		$L_{31} = 8.037 \text{ cm}$		$L_{41} = 2.364 \text{ cm}$					
$L_{5a} = 9.267 \text{ cm}$		$L_{5b} = 8.292 \text{ cm}$		$L_{6a} = 8.284 \text{ cm}$		$L_{6b} = 10.000 \text{ cm}$					
$\eta_c = 12.000^\circ$		$\gamma_c = 13.000^\circ$									

Table 4.5 Generated displacements for the Stephenson + linkage when $(\theta_{5ai})_g$ of Table 4.4 are used as input values.

i	θ_{12i}	$(\theta_{5ai})_d$	$(\theta_{5ai})_g$	$(\theta_{22i})_g$	$(\theta_{31i})_g$	$(\theta_{41i})_d$	$(\theta_{41i})_g$	e_i	μ_{1i}	μ_{2i}
1	0.000	43.356	43.356	55.950	-64.493	-5.000	-10.421	-5.421	12.594	54.072
2	30.000	15.525	15.525	32.490	-85.426	-60.000	-47.716	12.284	16.965	37.710
3	60.000	15.715	15.715	56.777	-67.387	12.000	9.928	-2.072	41.063	77.316
4	90.000	17.413	17.413	82.407	-55.964	55.000	53.600	-1.400	64.993	70.436
5	120.000	20.053	20.053	107.104	-47.096	90.000	90.246	0.246	87.051	42.658
6	150.000	24.236	24.236	129.328	-38.793	118.000	119.283	1.283	74.908	21.924
7	180.000	31.214	31.214	146.629	-28.799	130.000	132.883	2.883	64.586	18.318
8	-150.000	42.154	42.154	156.341	-19.244	140.000	134.022	-5.978	65.814	26.734
9	-120.000	56.210	56.210	158.169	-12.971	130.000	129.894	-0.106	78.041	37.136
10	-90.000	70.474	70.474	153.347	-10.167	118.000	119.478	1.478	82.874	50.355
11	-60.000	80.676	80.676	140.983	-12.851	100.000	101.325	1.325	60.308	65.824
12	-30.000	78.220	78.220	114.401	-26.397	70.000	69.285	-0.715	36.182	84.318
$e_{avg} = 2.933^\circ$		$e_{rms} = 4.442^\circ$								
$L_{12} = 4.500 \text{ cm}$		$L_{22} = 5.600 \text{ cm}$		$L_{31} = 7.984 \text{ cm}$		$L_{41} = 2.476 \text{ cm}$				
$L_{5a} = 9.267 \text{ cm}$		$L_{5b} = 8.118 \text{ cm}$		$L_{6a} = 8.284 \text{ cm}$		$L_{6b} = 10.000 \text{ cm}$				
$\eta_c = 12.000^\circ$		$\gamma_c = 13.000^\circ$								

Table 4.6 Desired and generated co-ordinates of the path for the Stephenson linkage in Example 3.

i	$(p_i)_d$	$(p_i)_g$	$(\delta_i)_d$	$(\delta_i)_g$	e_{xi}	e_{yi}	
	(cm)	(cm)	($^\circ$)	($^\circ$)	(cm)	(cm)	
1	75.000	74.769	12.000	10.593	0.134	-1.849	
2	73.000	72.507	5.000	2.126	-0.265	-3.673	
3	67.000	68.336	18.000	18.687	1.012	1.191	
4	67.000	67.155	49.000	50.781	-1.495	1.462	
5	71.000	70.935	82.000	83.060	-1.310	0.106	
6	78.000	77.702	106.000	107.256	-1.549	-0.773	
7	85.000	84.652	126.000	125.062	1.332	0.524	
8	92.000	90.042	139.000	138.648	1.842	-0.868	
9	94.000	93.107	149.000	148.870	0.874	-0.279	
10	94.000	93.869	156.000	155.863	0.212	0.152	
11	94.000	92.685	161.000	159.718	1.940	1.525	
12	88.000	89.853	159.000	160.548	-2.569	-1.614	
13	84.000	85.791	157.000	158.130	-2.295	-0.864	
14	78.000	81.234	152.000	151.802	-2.723	1.766	
15	78.000	77.163	141.000	140.652	0.947	-0.163	
16	77.000	74.437	126.000	123.565	4.104	-0.270	
17	72.000	73.109	96.000	97.386	-1.873	0.896	
18	73.000	73.126	51.000	53.771	-2.722	2.256	
$e_{avg} = 2.746 \text{ cm}$		$e_{rms} = 2.382 \text{ cm}$					

Table 4.7 Generated displacements for the Stephenson-I linkage in Example 3 for path generation.

i	θ_{12i}	$(\theta_{5ai})_d$	$(\theta_{5ai})_g$	$(\theta_{22i})_g$	$(\theta_{31i})_g$	$(\theta_{41i})_g$	μ_{1i}	μ_{2i}
1	0.000	39.500	39.502	66.147	-78.123	-36.762	26.645	41.361
2	20.000	19.600	19.744	57.338	-85.532	-47.626	37.594	37.906
3	40.000	10.300	10.328	62.440	-64.820	-32.383	52.113	32.436
4	60.000	5.600	5.611	73.242	-30.959	2.418	67.631	33.377
5	80.000	3.300	3.266	86.380	-2.876	40.165	83.113	43.041
6	100.000	2.500	2.487	100.330	13.458	70.960	82.158	57.502
7	120.000	3.200	3.155	114.105	22.525	95.840	69.049	73.314
8	140.000	5.600	5.620	126.737	28.075	116.042	58.884	87.967
9	160.000	10.600	10.595	137.099	32.458	131.034	53.495	81.425
10	180.000	18.700	18.662	144.287	37.257	139.502	54.376	77.756
11	-160.000	29.500	29.547	148.299	42.744	141.343	61.248	81.401
12	-140.000	42.200	42.230	149.855	47.769	137.937	72.376	89.831
13	-120.000	55.600	55.618	149.588	50.692	130.530	86.030	79.838
14	-100.000	68.700	68.723	147.686	49.878	119.539	78.964	69.661
15	-80.000	80.400	80.364	143.763	43.781	104.763	63.399	60.982
16	-60.000	88.500	88.456	136.474	30.957	85.263	48.018	54.307
17	-40.000	88.300	88.246	122.341	8.523	57.006	34.094	48.483
18	-20.000	70.500	70.429	95.440	-32.623	9.709	25.011	42.332
L_{12}	= 60.000 cm	L_{22}	= 85.674 cm	L_{31}	= 58.333 cm	L_{41}	= 51.704 cm	
L_{5a}	= 89.685 cm	L_{5b}	= 78.949 cm	R_A	= 99.459 cm	R_F	= 21.863 cm	
R_E	= 5.316 cm	a	= 40.533 cm					
γ_c	= -20.000°	α_A	= 180.000°	α_F	= -103.000°	α_E	= 0.000°	

Table 4.8 Desired and generated co-ordinates of the path for the Watt-II linkage in Example 4 for motion of the garage-door.

i	$(p_i)_d$ (cm)	$(p_i)_g$ (cm)	$(\delta_i)_d$ (°)	$(\delta_i)_g$ (°)	e_{xi} (cm)	e_{yi} (cm)
1	41.000	42.684	108.000	107.718	-0.320	1.666
2	40.000	39.911	102.838	102.190	0.460	0.011
3	39.100	37.910	94.100	94.516	-0.189	-1.208
4	39.100	37.423	85.900	85.881	-0.107	-1.674
5	40.000	38.354	77.162	78.039	-0.939	-1.479
6	41.000	40.085	72.000	71.707	-0.088	-0.934
7	43.000	42.466	65.091	66.019	-0.851	-0.199
8	45.000	46.339	60.073	59.357	1.168	0.868
9	47.000	49.389	56.077	55.137	2.002	1.525
10	51.000	54.182	49.881	49.366	2.421	2.117
11	54.000	59.038	46.238	44.012	5.110	2.020
12	57.000	62.538	43.173	40.248	6.163	1.406
13	62.000	63.146	38.979	39.595	0.461	1.246
14	66.000	64.722	36.221	37.895	-2.171	0.754
15	70.000	66.225	33.858	36.266	-4.733	0.175
16	73.000	69.441	32.293	32.772	-3.321	-1.412
e_{avg} = 3.075 cm				e_{rms} = 2.995 cm		

Table 4.9 Desired and generated displacements for the Watt-II linkage in Example 4 for motion of the garage-door.

i	$(\theta_{21i})_g$	$(\theta_{5ai})_d$	$(\theta_{5ai})_g$	$(\theta_{6ai})_g$	$(\theta_{31i})_g$	$(\theta_{41i})_d$	$(\theta_{41i})_g$	e_i	μ_{1i}	μ_{2i}	
1	-114.455	8.092	8.095	66.970	67.794	9.000	7.108	-1.892	57.450	60.687	
2	-111.763	7.761	7.763	59.951	60.770	6.000	6.642	0.642	60.474	54.127	
3	-108.772	6.093	6.094	51.045	51.876	4.000	4.815	0.815	65.134	47.061	
4	-105.923	2.823	2.823	41.041	41.909	0.000	1.376	1.375	71.254	40.534	
5	-103.549	-1.575	-1.576	31.133	32.058	-4.000	-3.188	0.812	78.027	35.246	
6	-101.680	-6.421	-6.422	22.015	23.007	-9.000	-8.187	0.813	84.742	31.194	
7	-100.000	-12.063	-12.064	12.583	13.659	-14.000	-13.992	0.008	87.937	27.651	
8	-98.018	-20.601	-20.601	-0.361	0.857	-22.000	-22.768	-0.768	77.416	23.625	
9	-96.761	-27.213	-27.213	-9.717	-8.377	-28.000	-29.568	-1.568	69.548	21.192	
10	-95.061	-37.731	-37.732	-23.853	-22.289	-38.000	-40.406	-2.406	57.329	18.117	
11	-93.516	-48.764	-48.764	-38.013	-36.170	-48.000	-51.813	-3.813	44.752	15.643	
12	-92.439	-57.039	-57.038	-48.294	-46.210	-56.000	-60.401	-4.401	35.401	14.191	
13	-92.251	-58.505	-58.505	-50.087	-47.958	-61.000	-61.925	-0.925	33.746	13.967	
14	-91.757	-62.352	-62.352	-54.747	-52.496	-67.000	-65.925	1.075	29.405	13.429	
15	-91.270	-66.073	-66.073	-59.183	-56.815	-73.000	-69.794	3.206	25.198	12.979	
16	-90.124	-74.115	-74.117	-68.405	-65.819	-81.000	-78.111	2.889	16.007	12.292	
$e_{avg} = 1.713^\circ$		$e_{rms} = 2.110^\circ$									
$L_{11} = 44.933 \text{ cm}$		$L_{21} = 37.614 \text{ cm}$		$L_{31} = 26.177 \text{ cm}$		$L_{41} = 22.574 \text{ cm}$					
$L_{5a} = 22.108 \text{ cm}$		$L_{5b} = 0.426 \text{ cm}$		$L_{6a} = 15.000 \text{ cm}$		$L_{6b} = 41.446 \text{ cm}$					
$R_A = 46.976 \text{ cm}$		$R_B = 64.681 \text{ cm}$		$\alpha = 76.221 \text{ cm}$		$\psi = 9.000^\circ$		$\varepsilon = 351.000^\circ$			
$\gamma_c = -20.000^\circ$		$\eta_c = 0.000^\circ$		$\alpha_A = 0.000^\circ$		$\alpha_B = 44.000^\circ$					

Table 4.10 Generated co-ordinates of the path for the Watt-II linkage in Example 4 for motion of the garage-door, with $L_{5b} = 0 \text{ cm}$.

i	$(p_i)_d$	$(p_i)_g$	$(\delta_i)_d$	$(\delta_i)_g$	e_{xi}	e_{yi}	
	(cm)	(cm)	($^\circ$)	($^\circ$)	(cm)	(cm)	
1	41.000	41.430	108.000	108.319	-0.352	0.337	
2	40.000	38.621	102.838	102.669	0.418	-1.319	
3	39.100	36.593	94.100	94.813	-0.274	-2.536	
4	39.100	36.097	85.900	85.990	-0.271	-2.992	
5	40.000	37.032	77.162	78.029	-1.207	-2.774	
6	41.000	38.773	72.000	71.652	-0.465	-2.192	
7	43.000	41.168	65.091	65.972	-1.348	-1.400	
8	45.000	45.066	60.073	59.374	0.508	-0.219	
9	47.000	48.144	56.077	55.220	1.233	0.543	
10	51.000	53.000	49.881	49.552	1.521	1.333	
11	54.000	57.953	46.238	44.287	4.136	1.466	
12	57.000	61.549	43.173	40.569	5.184	1.030	
13	62.000	62.175	38.979	39.922	-0.514	0.901	
14	66.000	63.804	36.221	38.236	-3.129	0.489	
15	70.000	65.361	33.858	36.614	-5.666	-0.017	
16	73.000	68.709	32.293	33.118	-4.161	-1.460	
$e_{avg} = 3.212 \text{ cm}$		$e_{rms} = 3.079 \text{ cm}$					

Table 4.11 Generated displacements for the Watt-II linkage in Example 4 for motion of the garage-door, with $L_{5b} = 0\text{cm}$.

i	$(\theta_{21i})_g$	$(\theta_{5ai})_d$	$(\theta_{5ai})_g$	$(\theta_{6ai})_g$	$(\theta_{31i})_g$	$(\theta_{41i})_d$	$(\theta_{41i})_g$	e_i	μ_{1i}	μ_{2i}
1	-114.496	7.000	8.014	66.970	67.802	9.000	8.108	-0.892	57.490	59.695
2	-111.803	7.000	7.686	59.951	60.781	6.000	7.643	1.643	60.511	53.138
3	-108.809	6.000	6.022	51.045	51.892	4.000	5.816	1.816	65.169	46.076
4	-105.957	4.000	2.756	41.041	41.931	0.000	2.374	2.374	71.287	39.557
5	-103.579	0.000	-1.639	31.133	32.087	-4.000	-2.194	1.806	78.060	34.281
6	-101.707	-6.000	-6.483	22.015	23.043	-9.000	-7.200	1.800	84.776	30.243
7	-100.024	-11.000	-12.123	12.583	13.705	-14.000	-13.015	0.985	87.901	26.720
8	-98.036	-20.000	-20.661	-0.361	0.920	-22.000	-21.811	0.189	77.375	22.731
9	-96.775	-30.000	-27.274	-9.717	-8.298	-28.000	-28.631	-0.631	69.501	20.333
10	-95.068	-40.000	-37.798	-23.853	-22.181	-38.000	-39.508	-1.508	57.270	17.327
11	-93.512	-50.000	-48.841	-38.013	-36.024	-48.000	-50.971	-2.971	44.671	14.947
12	-92.424	-55.000	-57.131	-48.294	-46.030	-56.000	-59.612	-3.612	35.293	13.582
13	-92.233	-58.000	-58.601	-50.087	-47.772	-61.000	-61.147	-0.147	33.633	13.375
14	-91.731	-63.000	-62.460	-54.747	-52.295	-67.000	-65.177	1.823	29.271	12.883
15	-91.234	-67.000	-66.196	-59.183	-56.599	-73.000	-69.078	3.922	25.038	12.479
16	-90.049	-70.000	-74.305	-68.405	-65.587	-81.000	-77.478	3.522	15.743	11.892
$e_{avg} = 1.853^\circ$		$e_{rms} = 2.174^\circ$								
$L_{11} = 44.933\text{ cm}$		$L_{21} = 37.614\text{ cm}$		$L_{31} = 26.177\text{ cm}$		$L_{41} = 22.574\text{ cm}$				
$L_{5a} = 22.108\text{cm}$		$L_{5b} = 0.000\text{ cm}$		$L_{6a} = 15.000\text{ cm}$		$L_{6b} = 41.446\text{ cm}$				
$R_A = 46.976\text{ cm}$		$R_B = 64.681\text{ cm}$		$a = 76.221\text{ cm}$		$\psi = 9.000^\circ$		$\varepsilon = 351.000^\circ$		
$\gamma_c = -20.000^\circ$		$\eta_c = 0.000^\circ$		$\alpha_A = 0.000^\circ$		$\alpha_B = 44.000^\circ$				

Chapter 5

Optimization of Transmission Angle for Planar Four-Bar Linkages

5.1 Introduction

As stated in Chapter 1, the present chapter is an extension of the work done by Dubey [1] which covered the function generation and path generation problems for planar four-bar linkage. In this chapter, the solutions obtained in reference [1] have been optimized from the view point of best transmission angle. Before going into the details of the optimization method, a brief note on transmission angle and its usefulness is given.

5.2 Transmission Angle

Before actually building a linkage, it is useful to have a measure of how well a linkage may perform while it is still in kinematic skeleton form on the drawing board or on the computer screen. Hartenberg and Denavit [7] gave a term "*run*" which formally means the effectiveness with which motion is imparted to the output link. It implies a smooth operation, in which a maximum force component is available to produce a torque or a force, whatever the case might be, in the output link. Though, a test on a kinematic

model checks out only an approximation of the static forces and tells nothing about the dynamic forces, however, some evaluation is better than none. Transmission angle is taken as a measure of the *run*.

Alt defined the transmission angle, μ , as the smaller (acute) angle between the direction of the velocity-difference vector \vec{V}_{CB} of the floating link and direction of the absolute velocity vector \vec{V}_C of the output link both taken at the point of connection. The transmission angle is illustrated in Figure 5.1. Since the velocity vectors are perpendicular to their respective links, the transmission angle is also given by the angle between the floating link (\vec{L}_3) and the output link (\vec{L}_4) as shown in Figure 5.2. Clearly the optimum value of μ is 90° ; the recommended range is $\mu \geq 30^\circ$.

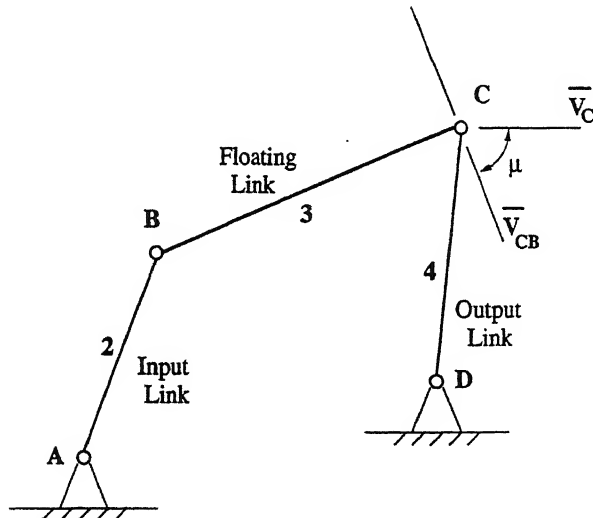


Figure 5.1: Transmission angle μ of a four-bar linkage.

Hence, it is always desirable to have the value of transmission angle more than 30° . The next section describes the optimization process as applied to the function generating linkages.

5.3 Optimization for Function Generation

The four-bar linkage for function generation is as shown in Figure 5.3. Link 2 is the input link and link 4 is the output link. The governing loop-closure equation is given by

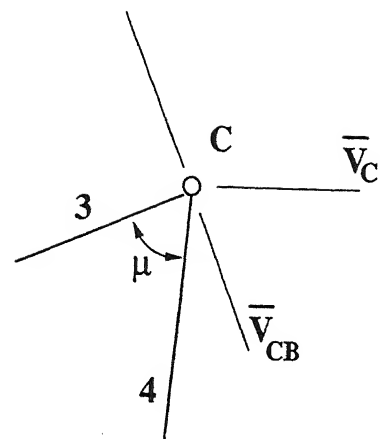


Figure 5.2: Transmission angle μ as the acute angle between link 3 and link 4.

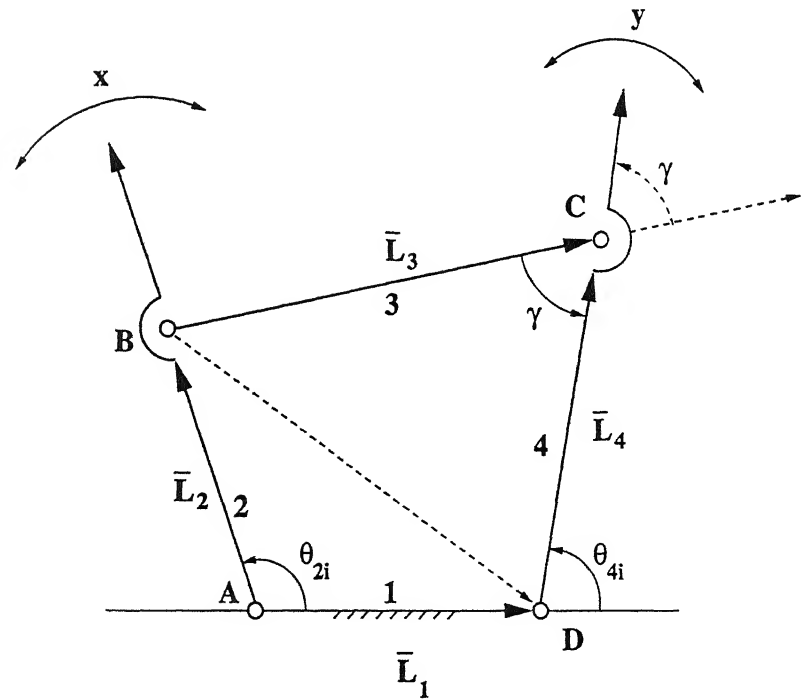


Figure 5.3: Four-bar linkage at the i^{th} design position when generating a function.

$$\vec{L}_1 + \vec{L}_4 - \vec{L}_2 - \vec{L}_3 = 0. \quad (5.1)$$

Equation (5.1) after elimination of θ_3 , at i^{th} design position gives

$$L_1^2 + L_2^2 + L_4^2 - L_3^2 - 2.L_1.L_2 \cos(\theta_{2i}) + 2.L_1.L_4 \cos(\theta_{4i}) - 2.L_2.L_4 \cos(\theta_{2i} - \theta_{4i}) = 0. \quad (5.2)$$

Dividing Equation (5.2) by $2.L_2.L_4$ one gets

$$D_1\mu_{1i} + D_2\mu_{2i} + D_3\mu_{3i} - \nu_i = 0 \quad (5.3)$$

where,

$$D_1 = \frac{L_1}{L_4}, \quad D_2 = \frac{L_1}{L_2}, \quad D_3 = \frac{L_1^2 + L_2^2 + L_4^2 - L_3^2}{2.L_2.L_4},$$

$$\mu_{1i} = \cos(\theta_{2i}), \quad \mu_{2i} = -\cos(\theta_{4i}), \quad \mu_{3i} = -1,$$

$$\nu_i = -\cos(\theta_{2i} - \theta_{4i}).$$

The value of L_1 is specified. θ_{2i} and θ_{4i} are obtained from the given function to be generated (i.e., x and $y = f(x)$).

Referring to Figure (5.3), it is seen that γ is the angle which \vec{L}_4 makes with \vec{L}_3 . It follows that,

$$BD^2 = AB^2 + AD^2 - 2.AB.AD \cos(\theta_{2i}) = BC^2 + DC^2 - 2.BC.DC \cos(\gamma_i)$$

or

$$\cos(\gamma_i) = \frac{BC^2 + DC^2 - AB^2 - AD^2 + 2.AB.AD \cos(\theta_{2i})}{2.BC.DC}$$

or

$$\cos(\gamma_i) = \frac{L_3^2 + L_4^2 - L_2^2 - L_1^2 + 2.L_2.L_1 \cos(\theta_{2i})}{2.L_3.L_4}$$

which gives (using Equation (5.3)),

$$\cos(\gamma_i) = \frac{2.L_4^2 - 2.L_2.L_4.D_3 + 2.L_2.L_1 \cos(\theta_{2i})}{2.L_3.L_4}.$$

Since μ is the acute angle between \vec{L}_3 and \vec{L}_4 , it follows that,

$$30^\circ \leq \gamma_i \leq (180^\circ - 30^\circ)$$

or

$$30^\circ \leq \gamma_i \leq 150^\circ$$

which can be written as

$$\gamma_i - 30^\circ \geq 0$$

and

$$-\gamma_i + 150^\circ \geq 0.$$

It should be noted that L_3 is given by $\sqrt{L_1^2 + L_2^2 + L_4^2 - 2.L_2.L_4.D_3}$ (from Equation (5.3)) and for L_3 to have a real magnitude, the terms under the square root should give a positive value. Taking, $\chi = L_1^2 + L_2^2 + L_4^2 - 2.L_2.L_4.D_3$, the condition is written as,

$$\chi \geq 0.$$

The optimization problem, is formulated as follows:

Minimize

$$f(D_1, D_2, D_3) = \sum_{i=1}^N (D_1\mu_{1i} + D_2\mu_{2i} + D_3\mu_{3i} - \nu_i) \quad (5.4)$$

subject to

$$D_1 \neq 0,$$

$$D_2 \neq 0,$$

$$\gamma_i - 30^\circ \geq 0,$$

$$-\gamma_i + 150^\circ \geq 0,$$

$$\chi \geq 0,$$

where i represents the number of the design positions and all other variables have their designated meanings. The first two constraints are necessary else (with reference to Equation (5.3)) L_2 and L_4 will become indefinite. If the Grashofian condition is to be satisfied and L_2 is to be the crank, then the following constraints are also included,

$$L_1 - L_2 \geq 0,$$

$$L_3 - L_2 \geq 0,$$

$$L_4 - L_2 \geq 0,$$

$$L_1 + L_2 + L_3 + L_4 - 2(L_2 + L_{max.}) \geq 0.$$

The objective function is a linear function, but the constraints, particularly, the constraint on the transmission angle, turn out to be highly nonlinear, making the optimization problem a nonlinear problem. Two approaches have been used for optimization, the Cauchy's steepest descent method and the Random search method.

Both the optimization methods need a start value i.e., some initial values of D_1, D_2, D_3 . The initial values are provided by solving the objective function without considering the constraints, using LSM. The search region for D_1, D_2, D_3 , when the constraints are included, has many local optima. This implies that the solution for the constrained problem will tend to localize near the initial values, but, this is certainly a better approach than giving arbitrary initial values.

Moreover, the limit on optimization of the transmission angle is not kept 30° at starting. This is explained as follows. Suppose that a linkage obtained from solving the unconstrained problem using LSM results in a minimum transmission angle of 17° . The constraint put on the transmission angle is then the nearest higher multiple of 5, which in this case is 20° . The reason for this stems from the fact that a higher value of trans-

mission angle as the constraint, makes the optimization unstable. Unstable optimization means, random wandering of the search direction in case of the steepest descent method and insufficient region and insufficient number of random solutions in case of the Random search method.

The optimization is carried out till an optimum value of 30° or more is reached or up to the value, after which no improvement is possible. A limit is always set on the maximum number of iterations as well as the maximum number of random generations.

The basic algorithms of the Cauchy's steepest descent method and Random search method are available in reference [14]. These algorithms were then modified for the linkage synthesis application. In the steepest descent method, the *Bracket Operator Penalty* is used. The multi-variable constrained problem is then reduced to a single variable unconstrained problem, which is solved by using the *Bounding Phase Method* and the *Golden Section Search Method*. In the random search method, random values of D_1, D_2, D_3 are generated near the region of the initial values of D_1, D_2, D_3 . The search region is increased, discarding the previous search region, up to a particular limit in case the solution is not found.

A point to be noted that, if the initial values of D_1, D_2, D_3 (obtained by the LSM) gave good function generation results (i.e., very less value of error in function generation), then there is a great chance that the function generation error will increase after maximizing the transmission angle.

A question arises that in cases where a crank was required for input, why the Grashofian condition was not incorporated during the LSM. The answer for this is that in the LSM, inclusion of constraints is not at all possible. If the solution is non-Grashofian, it is neglected and the LSM is again applied with changed initial values. But in the optimization of transmission angle, whether it is Cauchy's steepest descent method or Random search method, the values of D_1, D_2, D_3 and hence the link-lengths continuously change during the search. It is possible for the search to enter into the non-Grashofian zone. Therefore,

the Grashofian condition is taken as a constraint to penalize the objective function. It is possible that, within the limit on the maximum number of iterations, no solution emerges or, within the region of search, no solution exists.

5.4 Optimization for Path Generation

This section gives the optimization problem formulation only, without going into the details. The four-bar linkage for path generation is shown in Figure 5.4. There are two

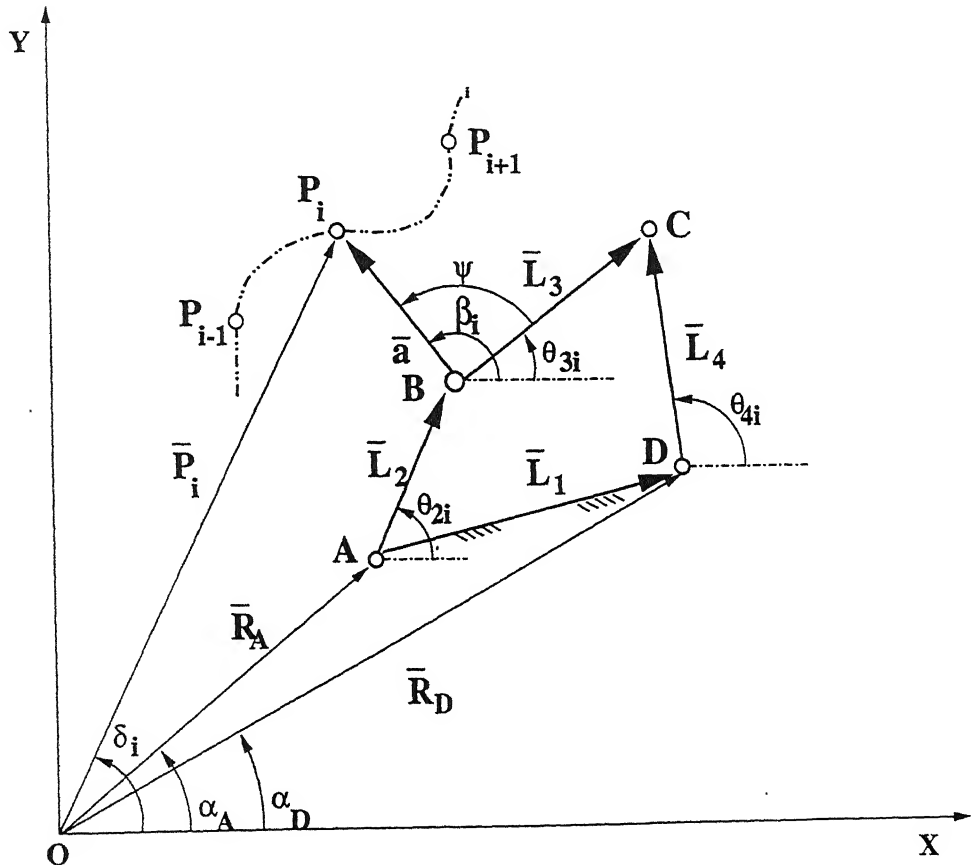


Figure 5.4: Four-bar linkage at the i^{th} design position when generating a path.

loops, $OABPO$ and $ABCFA$ from which the following equations are derived,

$$D_1\mu_{1i} + D_2\mu_{2i} + D_3\mu_{3i} - D_1D_2\rho_i - \nu_i = 0 \quad (5.5)$$

where,

$$D_1 = R_A, D_2 = L_2, D_3 = L_2^2 + R_2^2 - a^2, \lambda = D_1 D_2 = R_A \cdot L_2$$

$$\mu_{1i} = -2 \cdot P_i \cos(\alpha_A - \delta_i),$$

$$\mu_{2i} = -2 \cdot P_i \cos(\theta_{2i} - \delta_i), \mu_{3i} = 1,$$

$$\rho_i = -2 \cos(\alpha_A - \theta_{2i}), \nu_i = -P_i^2$$

and

$$D'_1 \mu'_{1i} + D'_2 \mu'_{2i} + D'_3 \mu'_{3i} - D'_1 D'_2 \rho'_i - \nu'_i = 0 \quad (5.6)$$

where,

$$D'_1 = R_D, D'_2 = L_3, D'_3 = R_A^2 + L_2^2 + R_D^2 + L_3^2 - L_4^2,$$

$$\mu'_{1i} = -2 \cdot R_A \cos(\alpha_A - \alpha_D) - 2 \cdot L_2 \cos(\theta_{2i} - \alpha_D),$$

$$\mu'_{2i} = 2 \cdot R_A \cos(\alpha_A - \theta_{3i}) + 2 \cdot L_2 \cos(\theta_{2i} - \theta_{3i}), \mu'_{3i} = 1,$$

$$\rho'_i = 2 \cos(\theta_{3i} - \alpha_D),$$

$$\nu'_i = -R_A \cdot L_2 \cos(\alpha_A - \theta_{2i}).$$

α_A and α_D are assumed and θ_{2i} , \vec{P}_i (P_i with δ_i) are specified. Using LSM, the unconstrained problem is solved to give the values of D_1, D_2, D_3 and D'_1, D'_2, D'_3 and hence the link-lengths.

For the constrained problem, the constraints are just the same as that for the function generation problem. The objective function constitutes *only* Equation (5.6) and *not* Equation (5.5). An objective function constituting both the equations could be taken and represented as follows:

Minimize

$$\sum_{i=1}^N f(D_1, D_2, D_3) + \sum_{i=1}^N f'(D'_1, D'_2, D'_3),$$

but then it would be a problem of six variables. Moreover there would be unnecessary effects of $\sum f$ and $\sum f'$ on each other, making the optimization process very complex. Further, taking Equation (5.5) as objective function will change the length of L_2 which is obtained minimizing the error in the loop $OABPO$ involving \vec{P}_i s. Any change in L_2 can

increase the error in the path generated. Therefore, only Equation (5.6) is taken as the objective function and one can write

Minimize

$$f' (D'_1, D'_2, D'_3) = \sum_{i=1}^N (D'_1 \mu'_{1i} + D'_2 \mu'_{2i} + D'_3 \mu'_{3i} + D'_1 D'_2 \rho'_i - \nu'_i) \quad (5.7)$$

The initial values of D'_1, D'_2, D'_3 are obtained from the unconstrained LSM solution. Both the methods of optimization, the Cauchy's method and Random search method are used for path generation also.

5.5 Numerical Examples

Two examples are given which show the application of the optimization of transmission angle on the four-bar linkage.

Example 1: A crank-rocker example was illustrated in Dubey [1] (p. 50), to show the application of least square method to function generation of four-bar linkage. The synthesized linkage had a very poor minimum transmission angle $\mu_{min} = 17.685^\circ$.¹ The values of the error in the generated function were given by $e_{avg} = 5.250^\circ$ and $e_{rms} = 6.914^\circ$.

The same data is taken as the input for the present program. The value of L_1 is taken as 10 cm. Table 5.1 shows the desired and generated values of the displacements of the resulting linkage. The Cauchy's steepest descent method and Random search method are applied separately to maximize μ_{min} . Table 5.2(a) gives the values of the displacements generated and the dimensions obtained when the linkage is optimized for $\mu_{min} = 20^\circ$, using Cauchy's steepest descent method. The value of μ_{min} obtained is 19.995° . It is seen that there is change in errors generated at each design position. In Table 5.2(b) the linkage is optimized for 25° and in Table 5.2(c) for 30° . The final values of error obtained are

¹Due to different program codings and different numerical accuracy maintained therein, the values of angles generated by the present program and Dubey's [1] program differ upto a maximum of 3° . Dubey [1] (Plot 3.4, p. 60) reported $\mu_{min} = 14.83^\circ$.

$e_{avg} = 7.794^\circ$ and $e_{rms} = 9.008^\circ$. The optimized value of μ_{min} is 30.000° . Tables 5.3(a) and 5.3(b) give the values obtained using Random search method. No further improvement is obtained after $\mu_{min} = 25.245^\circ$. The solutions obtained by both the methods differ from each other. Moreover, time taken by Random search method is more as compared to Cauchy's method. The reason for this is the large number of search points generated in the Random search method.

It follows that both the methods improve the minimum transmission angle of the linkage at the same time increasing the error in the function generated. At this stage it can not be said which method is the better one. If Random search method fails to improve μ_{min} up to 30° , then Cauchy's method gives a large error of 18.599° , at the 1st design position, for $\mu_{min} = 30^\circ$.

Example 2: A four-bar linkage, shown in Figure 5.5, is used to generate a path whose coordinates are given in Table 5.4. Crank AB is the input link. The specified values are $\alpha_A = 120^\circ$, $\alpha_D = 25^\circ$ and $\psi = -22^\circ$. The errors in the synthesized linkage are given by $e_{avg} = 0.025$ cm and $e_{rms} = 0.052$ cm. The transmission angle has a minimum value of $\mu_{min} = 23.249^\circ$.

Tables 5.5(a) and 5.5(b) give the values of the displacements and μ_{min} obtained using Cauchy's steepest descent method. The final values obtained are $e_{avg} = 0.052$ cm, $e_{rms} = 0.138$ cm and $\mu_{min} = 30.000^\circ$. Tables 5.6(a) and 5.6(b) give the values obtained using Random search method. The values obtained are $e_{avg} = 0.046$ cm, $e_{rms} = 0.118$ cm and $\mu_{min} = 30.147^\circ$. Both the methods successfully optimized the minimum transmission angle but with increased error in the path generated.

From Table 5.5(a) it is seen that application of Cauchy's method for $\mu_{min} = 25^\circ$ results in decrease in values of errors to $e_{avg} = 0.009$ cm and $e_{rms} = 0.009$ cm.

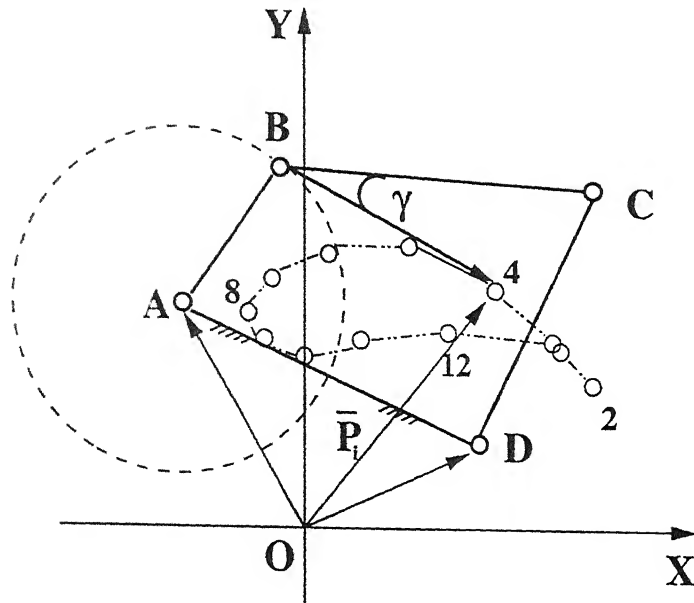


Figure 5.5: Four-bar linkage synthesized in Example 2 for path generation.

5.6 Conclusion

The optimization of the transmission angle leads to a linkage with acceptable aptness of run.

An ideal case would have been a high minimum transmission angle resulting from the unconstrained equation itself. But due to the initial assumptions and the various mathematical input-output relationships, this condition is attained in a very few cases only. The better option is to have more than one solution using LSM (by varying the set of initial assumptions) and subjecting them to optimization of transmission angle. The best solution obtained thereafter is the optimum solution.

The satisfactory performance of the optimization methods largely depend on the mathematical nature of the generated function and the arbitrary choices - starting angles and positions of hinges etc. When, even after application of both the methods, a poor transmission angle results, the only remedy is to redesign on different arbitrary choices.

The case of motion generation, though not considered in the present work, is just similar to path generation. The only difference is that in the loop $OABPO$ of Figure 5.4 instead

of θ_3 , θ_2 is eliminated.

Table 5.1 Desired and generated displacements for the four-bar linkage in Example 1 for function generation.

i	θ_{2i}	$(\theta_{3i})_g$	$(\theta_{4i})_d$	$(\theta_{4i})_g$	e_i	μ_i
1	15.000	13.852	30.000	31.538	1.538	17.685
2	60.000	12.990	50.000	47.814	-2.186	34.824
3	105.000	18.650	70.000	71.334	1.334	52.684
4	150.000	27.153	90.000	91.405	1.405	64.252
5	-165.000	37.854	110.000	103.891	-6.109	66.037
6	-120.000	48.393	100.000	105.848	5.848	57.454
7	-75.000	52.303	85.000	93.480	8.480	41.178
8	-30.000	37.486	75.000	59.897	-15.103	22.411
$e_{avg} = 5.250^\circ$		$e_{rms} = 6.914^\circ$				
$D_1 = 1.235$		$D_2 = 3.080$		$D_3 = -0.473$		
$L_1 = 10.000 \text{ cm}$		$L_2 = 3.247 \text{ cm}$		$L_3 = 14.176 \text{ cm}$		
$L_4 = 8.095 \text{ cm}$		$\mu_{min} = 17.685^\circ$				

Table 5.2(a) Generated displacements for the four-bar linkage in Example 1 obtained using Cauchy's steepest descent method for $\mu_{min} = 20^\circ$.

i	θ_{2i}	$(\theta_{3i})_g$	$(\theta_{4i})_d$	$(\theta_{4i})_g$	e_i	μ_i
1	15.000	17.539	30.000	37.534	7.534	19.995
2	60.000	15.213	50.000	50.309	0.309	35.096
3	105.000	20.314	70.000	71.979	1.977	51.665
4	150.000	28.559	90.000	91.051	1.051	62.492
5	-165.000	38.988	110.000	103.150	-6.849	64.163
6	-120.000	49.187	100.000	105.314	5.314	56.127
7	-75.000	52.964	85.000	93.914	8.914	40.950
8	-30.000	39.449	75.000	63.432	-11.568	23.983
$e_{avg} = 5.440^\circ$		$e_{rms} = 6.617^\circ$				
$D_1 = 1.189$		$D_2 = 3.188$		$D_3 = -0.456$		
$L_1 = 10.000 \text{ cm}$		$L_2 = 3.136 \text{ cm}$		$L_3 = 14.302 \text{ cm}$		
$L_4 = 8.407 \text{ cm}$		$\mu_{min} = 19.995^\circ$		$time = 1.480 \text{ s}$		

Table 5.2(b) Generated displacements for the four-bar linkage in Example obtained using Cauchy's steepest descent method for $\mu_{\min} = 25^\circ$.

i	θ_{2i}	$(\theta_{3i})_g$	$(\theta_{4i})_d$	$(\theta_{4i})_g$	e_i	μ_i
1	15.000	18.762	30.000	43.759	13.759	24.997
2	60.000	15.424	50.000	54.476	4.476	39.052
3	105.000	19.104	70.000	74.683	4.683	55.580
4	150.000	26.055	90.000	92.717	2.717	66.661
5	-165.000	35.223	110.000	103.610	-6.390	68.387
6	-120.000	44.178	100.000	104.304	4.304	60.126
7	-75.000	47.166	85.000	91.979	6.979	44.813
8	-30.000	36.002	75.000	64.539	-10.461	28.538
$e_{avg} = 6.721^\circ$		$e_{rms} = 7.551^\circ$				
$D_1 = 1.389$		$D_2 = 3.744$		$D_3 = -0.485$		
$L_1 = 10.000 \text{ cm}$		$L_2 = 2.671 \text{ cm}$		$L_3 = 13.326 \text{ cm}$		
$L_4 = 7.197 \text{ cm}$		$\mu_{\min} = 24.997^\circ$		$time = 1.540 \text{ s}$		

Table 5.2(C) Generated displacements for the four-bar linkage in Example obtained using Cauchy's steepest descent method for $\mu_{\min} = 30^\circ$.

i	θ_{2i}	$(\theta_{3i})_g$	$(\theta_{4i})_d$	$(\theta_{4i})_g$	e_i	μ_i
1	15.000	18.599	30.000	48.599	18.599	30.000
2	60.000	14.982	50.000	58.194	8.194	43.212
3	105.000	17.555	70.000	77.199	7.199	59.644
4	150.000	23.330	90.000	94.270	4.270	70.940
5	-165.000	31.277	110.000	103.990	-6.010	72.714
6	-120.000	39.021	100.000	103.278	3.278	64.256
7	-75.000	41.343	85.000	90.211	5.211	48.868
8	-30.000	32.190	75.000	65.406	-9.594	33.216
$e_{avg} = 7.794^\circ$		$e_{rms} = 9.008^\circ$				
$D_1 = 1.640$		$D_2 = 4.450$		$D_3 = -0.526$		
$L_1 = 10.000 \text{ cm}$		$L_2 = 2.247 \text{ cm}$		$L_3 = 12.515 \text{ cm}$		
$L_4 = 6.097 \text{ cm}$		$\mu_{\min} = 30.000^\circ$		$time = 2.370 \text{ s}$		

Table 5.3(a) Generated displacements for the four-bar linkage in Example obtained using Random search method for $\mu_{\min} = 20^\circ$.

i	θ_{2i}	$(\theta_{3i})_g$	$(\theta_{4i})_d$	$(\theta_{4i})_g$	e_i	μ_i
1	15.000	15.540	30.000	37.562	7.562	22.021
2	60.000	12.938	50.000	52.324	2.324	39.386
3	105.000	17.241	70.000	75.786	5.786	58.545
4	150.000	24.762	90.000	96.043	6.043	71.281
5	-165.000	34.917	110.000	108.187	-1.813	73.269
6	-120.000	45.362	100.000	109.129	9.129	63.767
7	-75.000	49.636	85.000	95.761	10.761	46.125
8	-30.000	36.774	75.000	63.395	-11.605	26.621
$e_{avg} = 6.878^\circ$		$e_{rms} = 7.662^\circ$				
$D_1 = 1.415$		$D_2 = 3.259$		$D_3 = -0.294$		
$L_1 = 10.000 \text{ cm}$		$L_2 = 3.068 \text{ cm}$		$L_3 = 13.119 \text{ cm}$		
$L_4 = 7.068 \text{ cm}$		$\mu_{\min} = 22.021^\circ$		$time = 23.170 \text{ s}$		

Table 5.3(b) Generated displacements for the four-bar linkage in Example obtained using Random search method for $\mu_{\min} = 25^\circ$.

i	θ_{2i}	$(\theta_{3i})_g$	$(\theta_{4i})_d$	$(\theta_{4i})_g$	e_i	μ_i
1	15.000	16.246	30.000	41.491	11.491	25.245
2	60.000	12.715	50.000	55.561	5.561	42.846
3	105.000	16.106	70.000	79.094	9.094	62.988
4	150.000	22.915	90.000	99.564	9.564	76.649
5	-165.000	32.662	110.000	111.465	1.465	78.803
6	-120.000	43.030	100.000	111.592	11.592	68.562
7	-75.000	47.538	85.000	97.409	12.409	49.872
8	-30.000	35.925	75.000	65.726	-9.274	29.800
$e_{avg} = 8.806^\circ$		$e_{rms} = 9.445^\circ$				
$D_1 = 1.560$		$D_2 = 3.405$		$D_3 = -0.148$		
$L_1 = 10.000 \text{ cm}$		$L_2 = 2.937 \text{ cm}$		$L_3 = 12.462 \text{ cm}$		
$L_4 = 6.410 \text{ cm}$		$\mu_{\min} = 25.245^\circ$		$time = 13.790 \text{ s}$		

No further improvement in μ_{\min} within the specified limits of the optimization zone.

Table 5.4 Desired and generated displacements for the four-bar linkage i

Example 2 for path generation.

i	$(p_i)_d$	$(p_i)_g$	$(\delta_i)_d$	$(\delta_i)_g$	e_{xi}	e_{yi}	θ_{2i}	$(\theta_{3i})_g$	$(\theta_{4i})_g$	μ_i	
	(cm)	(cm)	(°)	(°)	(cm)	(cm)	(°)	(°)	(°)	(°)	
1	3.779	3.787	33.790	33.752	0.008	0.002	-36.000	40.313	64.845	36.018	
2	3.994	3.887	25.670	23.612	-0.039	-0.173	-6.000	6.718	33.584	23.249	
3	3.867	3.863	34.050	34.145	-0.007	0.003	24.000	-5.294	38.354	29.448	
4	3.694	3.692	49.830	50.020	-0.011	0.006	54.000	-7.896	55.394	47.337	
5	3.560	3.558	67.970	67.675	0.016	-0.009	84.000	-6.827	74.944	66.970	
6	3.272	3.274	84.440	84.529	-0.005	0.002	114.000	-2.942	93.567	84.943	
7	2.969	2.970	97.860	97.889	-0.002	0.001	144.000	4.301	108.850	81.354	
8	2.588	2.588	105.370	105.352	0.001	0.000	174.000	15.459	118.966	74.913	
9	2.198	2.198	103.870	103.876	0.000	0.000	-156.000	29.783	123.516	77.743	
10	2.000	1.999	90.830	90.898	-0.002	-0.001	-126.000	45.053	122.987	88.901	
11	2.246	2.243	71.110	71.157	-0.003	-0.002	-96.000	57.810	116.787	74.497	
12	2.960	2.962	52.550	52.538	0.002	0.001	-66.000	61.221	100.700	55.224	
$e_{avg} = 0.025 \text{ cm}$		$e_{rms} = 0.052 \text{ cm}$									
$D_1 = -4.237$		$D_2 = 2.285$		$D_3 = 25.272$							
$L_1 = 3.901 \text{ cm}$		$L_2 = 2.180 \text{ cm}$		$L_3 = 4.237 \text{ cm}$		$L_4 = 3.386 \text{ cm}$					
$a = 2.983 \text{ cm}$		$\alpha_A = 120.000^\circ$		$\alpha_D = 25.000^\circ$		$\psi = -22.000^\circ$					
$R_A = 2.969 \text{ cm}$		$R_D = 2.285 \text{ cm}$		$\mu_{min} = 23.249^\circ$							

Table 5.5(a) Generated displacements for the four-bar linkage in Example obtained using Cauchy's steepest descent method for $\mu_{min} = 25^\circ$.

i	$(p_i)_d$	$(p_i)_g$	$(\delta_i)_d$	$(\delta_i)_g$	e_{xi}	e_{yi}	θ_{2i}	$(\theta_{3i})_g$	$(\theta_{4i})_g$	μ_i	
	(cm)	(cm)	(°)	(°)	(cm)	(cm)	(°)	(°)	(°)	(°)	
1	3.779	3.787	33.790	33.752	0.008	0.002	-36.000	43.673	70.223	37.657	
2	3.994	4.008	25.670	25.852	0.007	0.017	-6.000	10.488	38.630	25.001	
3	3.867	3.863	34.050	34.145	-0.007	0.003	24.000	-3.068	41.622	31.100	
4	3.694	3.692	49.830	50.020	-0.011	0.006	54.000	-6.644	58.031	49.082	
5	3.560	3.558	67.970	67.675	0.016	-0.009	84.000	-6.296	77.495	69.123	
6	3.272	3.274	84.440	84.529	-0.005	0.002	114.000	-3.038	96.299	87.682	
7	2.969	2.970	97.860	97.889	-0.002	0.001	144.000	3.707	111.826	77.988	
8	2.588	2.588	105.370	105.352	0.001	0.000	174.000	14.653	122.004	71.171	
9	2.198	2.198	103.870	103.876	0.000	0.000	-156.000	29.077	126.394	74.175	
10	2.000	1.999	90.830	90.898	-0.002	-0.001	-126.000	44.638	125.674	85.905	
11	2.246	2.243	71.110	71.157	-0.003	-0.002	-96.000	57.859	119.473	76.868	
12	2.960	2.962	52.550	52.538	0.002	0.001	-66.000	62.223	103.995	57.105	
$e_{avg} = 0.009 \text{ cm}$		$e_{rms} = 0.009 \text{ cm}$									
$D_1 = -4.163$		$D_2 = 2.376$		$D_3 = 25.274$							
$L_1 = 3.961 \text{ cm}$		$L_2 = 2.180 \text{ cm}$		$L_3 = 4.163 \text{ cm}$		$L_4 = 3.357 \text{ cm}$					
$a = 2.983 \text{ cm}$		$\alpha_A = 120.000^\circ$		$\alpha_D = 25.000^\circ$		$\psi = -22.000^\circ$					
$R_A = 2.969 \text{ cm}$		$R_D = 2.377 \text{ cm}$		$\mu_{min} = 25.001^\circ$		$time = 0.550 \text{ s}$					

Table 5.6(a), Generated displacements for the four-bar linkage in Example obtained using Cauchy's steepest descent method for $\mu_{\min} = 30^\circ$.

i	$(p_i)_d$	$(p_i)_d$	$(\delta_i)_d$	$(\delta_i)_g$	e_{xi}	e_{yi}	θ_{2i}	$(\theta_{3i})_g$	$(\theta_{4i})_g$	μ_i
	(cm)	(cm)	($^\circ$)	($^\circ$)	(cm)	(cm)	($^\circ$)	($^\circ$)	($^\circ$)	($^\circ$)
1	3.779	3.787	33.790	33.752	0.008	0.002	-36.000	50.600	82.901	42.698
2	3.994	4.276	25.670	31.040	0.064	0.475	-6.000	19.344	51.524	30.000
3	3.867	3.863	34.050	34.145	-0.007	0.003	24.000	2.209	50.568	36.021
4	3.694	3.692	49.830	50.020	-0.011	0.006	54.000	-4.071	65.548	54.647
5	3.560	3.558	67.970	67.675	0.016	-0.009	84.000	-5.912	85.093	76.283
6	3.272	3.274	84.440	84.529	-0.005	0.002	114.000	-4.732	104.832	82.868
7	2.969	2.970	97.860	97.889	-0.002	0.001	144.000	0.247	121.494	65.894
8	2.588	2.588	105.370	105.352	0.001	0.000	174.000	10.566	131.888	57.350
9	2.198	2.198	103.870	103.876	0.000	0.000	-156.000	25.633	135.385	61.165
10	2.000	1.999	90.830	90.898	-0.002	-0.001	-126.000	42.372	133.618	75.399
11	2.246	2.243	71.110	71.157	-0.003	-0.002	-96.000	57.060	126.936	84.871
12	2.960	2.962	52.550	52.538	0.002	0.001	-66.000	63.836	112.431	63.213

$$e_{avg} = 0.052 \text{ cm}$$

$$e_{rms} = 0.138 \text{ cm}$$

$$D_1 = -3.924$$

$$D_2 = 2.614$$

$$D_3 = 25.293$$

$$L_1 = 4.123 \text{ cm}$$

$$L_2 = 2.180 \text{ cm}$$

$$L_3 = 3.924 \text{ cm}$$

$$L_4 = 3.242 \text{ cm}$$

$$a = 2.983 \text{ cm}$$

$$\alpha_A = 120.000^\circ$$

$$\alpha_D = 25.000^\circ$$

$$\psi = -22.000^\circ$$

$$R_A = 2.969 \text{ cm}$$

$$R_D = 2.615 \text{ cm}$$

$$\mu_{\min} = 30.000^\circ$$

$$time = 1.430 \text{ s}$$

Table 5.6(a) Generated displacements for the four-bar linkage in Example obtained using Random search method for $\mu_{\min} = 25^\circ$.

i	$(p_i)_d$	$(p_i)_d$	$(\delta_i)_d$	$(\delta_i)_g$	e_{xi}	e_{yi}	θ_{2i}	$(\theta_{3i})_g$	$(\theta_{4i})_g$	μ_i
	(cm)	(cm)	($^\circ$)	($^\circ$)	(cm)	(cm)	($^\circ$)	($^\circ$)	($^\circ$)	($^\circ$)
1	3.779	3.787	33.790	33.752	0.008	0.002	-36.000	44.989	73.264	39.324
2	3.994	4.064	25.670	26.915	0.024	0.110	-6.000	12.288	41.645	26.479
3	3.867	3.863	34.050	34.145	-0.007	0.003	24.000	-2.171	43.865	32.643
4	3.694	3.692	49.830	50.020	-0.011	0.006	54.000	-6.470	60.196	51.049
5	3.560	3.558	67.970	67.675	0.016	-0.009	84.000	-6.775	79.950	71.816
6	3.272	3.274	84.440	84.529	-0.005	0.002	114.000	-4.171	99.237	88.691
7	2.969	2.970	97.860	97.889	-0.002	0.001	144.000	2.033	115.205	73.359
8	2.588	2.588	105.370	105.352	0.001	0.000	174.000	12.816	125.422	65.927
9	2.198	2.198	103.870	103.876	0.000	0.000	-156.000	27.473	129.420	69.215
10	2.000	1.999	90.830	90.898	-0.002	-0.001	-126.000	43.421	128.194	81.868
11	2.246	2.243	71.110	71.157	-0.003	-0.002	-96.000	57.081	121.608	79.914
12	2.960	2.962	52.550	52.538	0.002	0.001	-66.000	62.096	106.117	59.333

$$e_{avg} = 0.018 \text{ cm}$$

$$e_{rms} = 0.033 \text{ cm}$$

$$D_1 = -4.074$$

$$D_2 = 2.447$$

$$D_3 = 25.435$$

$$L_1 = 4.009 \text{ cm}$$

$$L_2 = 2.180 \text{ cm}$$

$$L_3 = 4.074 \text{ cm}$$

$$L_4 = 3.274 \text{ cm}$$

$$a = 2.983 \text{ cm}$$

$$\alpha_A = 120.000^\circ$$

$$\alpha_D = 25.000^\circ$$

$$\psi = -22.000^\circ$$

$$R_A = 2.969 \text{ cm}$$

$$R_D = 2.447 \text{ cm}$$

$$\mu_{\min} = 26.479^\circ$$

$$time = 26.700 \text{ s}$$

generated displacements for the four-bar linkage in Example 2 obtained using Random search method for $\mu_{\min} = 30^\circ$.

i	$(p_i)_d$ (cm)	$(p_i)_d$ (cm)	$(\delta_i)_d$ ($^\circ$)	$(\delta_i)_g$ ($^\circ$)	e_{xi} (cm)	e_{yi} (cm)	θ_{2i} ($^\circ$)	$(\theta_{3i})_g$ ($^\circ$)	$(\theta_{4i})_g$ ($^\circ$)	μ_i ($^\circ$)	
1	3.779	3.787	33.790	33.752	0.008	0.002	-36.000	49.192	81.707	43.121	
2	3.994	4.236	25.670	30.240	0.059	0.403	-6.000	17.969	50.334	30.147	
3	3.867	3.863	34.050	34.145	-0.007	0.003	24.000	1.155	50.027	36.304	
4	3.694	3.692	49.830	50.020	-0.011	0.006	54.000	-5.025	65.547	55.312	
5	3.560	3.558	67.970	67.675	0.016	-0.009	84.000	-6.937	85.563	77.417	
6	3.272	3.274	84.440	84.529	-0.005	0.002	114.000	-5.953	105.773	81.155	
7	2.969	2.970	97.860	97.889	-0.002	0.001	144.000	-1.196	122.826	63.502	
8	2.588	2.588	105.370	105.352	0.001	0.000	174.000	9.109	133.228	54.479	
9	2.198	2.198	103.870	103.876	0.000	0.000	-156.000	24.379	136.342	58.524	
10	2.000	1.999	90.830	90.898	-0.002	-0.001	-126.000	41.300	134.101	73.420	
11	2.246	2.243	71.110	71.157	-0.003	-0.002	-96.000	56.050	126.940	86.222	
12	2.960	2.962	52.550	52.538	0.002	0.001	-66.000	62.723	111.886	64.055	
$e_{avg} = 0.046$ cm		$e_{rms} = 0.118$ cm									
$D_1 = -3.903$		$D_2 = 2.618$		$D_3 = 25.606$							
$L_1 = 4.126$ cm		$L_2 = 2.180$ cm		$L_3 = 3.903$ cm		$L_4 = 3.170$ cm					
$a = 2.983$ cm		$\alpha_A = 120.000^\circ$		$\alpha_D = 25.000^\circ$		$\psi = -22.000^\circ$					
$R_A = 2.969$ cm		$R_D = 2.618$ cm		$\mu_{\min} = 30.147^\circ$		$time = 11.090$ s					

Chapter 6

Conclusions

In the present thesis, a software package for the synthesis, analysis and animation of planar six-bar linkages has been prepared. The synthesis of the four-bar linkage has been extended to include the consideration of transmission angle. The main conclusions that can be drawn from this work are summarized below:

1. The synthesis of the linkages have been carried out by using the **Least Square Error minimizing Optimization Method (LSM)** and the **Linear Superposition Technique**. The LSM is an efficient method. There is no limitation on the number of the design points and the structural error is optimized over the whole range of the linkage motion. The absence of iterative processes is an advantage of the method over other optimization methods. The present thesis covers Stephenson-I linkage for the function and path generation, and Watt-II linkage for the motion generation. The other linkages, viz., Stephenson-II and III and Watt-I can also be used for the synthesis process.

The LSM also has certain limitations. The major difficulty is finding a good set of values of the specified dimensions and the assumed values of the angular positions of the floating link (angle θ_{5a} , in all the three cases of the synthesis) at the design points.

Towards this end, coupler curve atlases for the planar six-bar linkages designating the angular positions of coupler links at certain reference positions will be very helpful.

2. The optimization of transmission angle for four-bar linkage gives a better linkage from the view point of motion and force transference. At the same time, error in the generated functions also increase. Both the methods, viz., Cauchy's steepest descent method and Random search method should be applied and the better solution should be accepted.
3. The dimensions of the linkages and the values of the error in the generated functions, known as *structural error*, were given up to the third place of decimal. An additional error, known as *mechanical error*, due to deflections of the links, play in the joints, and manufacturing tolerances, will inevitably occur in addition to structural error in any actual linkage. Hence, depending on the need and practicality, the level of accuracy in the dimensions should be taken.
4. The analysis of linkages is based on the analytical approach where the loop closure equations of the linkages are used. Each equation gives rise to two scalar equations by taking the x and y components separately. The resulting equations are then used for displacement analysis. The time derivatives of the equations are used for velocity and acceleration analysis. The software provides many options for the analysis, which are given in Appendix A.
5. The animation of the linkages provide a better understanding of the actual motion of the linkages. The stationary configurations and the displacement zone of the linkages can be easily seen from the animation.
6. In Chapter 2, it was stated, and supported with examples, that six-bar linkages have many advantages over the four-bar linkages. Hunt [4] (pp. 224 - 34) cites certain examples of the six-bar linkages, where complex motion is generated by them, but

with poor transmission angles. The planar six-bar linkages provide a fruitful field for further investigation.

6.1 Suggestions for Future Work

The following directions may be taken up to extend the work carried out in the present thesis:

1. Weighted error function can be used in the synthesis processes, where the critical design points can have more weightage than the other design points. (The weightage error function for planar four-bar linkages was applied by Dubey [1].)
2. The optimization of transmission angles for six-bar linkage can also be pursued. The problem becomes more complex than the four-bar linkage as there are two transmission angles and more loops-closure equations involved.
3. Tolerance Analysis can be included, which will give an indication of the magnitude of mechanical errors. In the software, the dimensions and angular positions of the linkages are given up to three places after the decimal point. This can be controlled up to the accuracy really possible.
4. An atlas of the coupler curves of all the linkages with varying dimension ratios can be obtained, which can be treated as a guide for the designers.
5. The dynamics of linkages should be included, so as to make the package more useful. The design of linkages depends to a great extent on the dynamics involved in the motion.
6. The package should be ported to Windows environment, so as to have all the facilities and tools of a commercially available software package. This is being currently attempted as a part of the same DST project.

Bibliography

- [1] Dubey, N. K., "Computer Aided Synthesis and Animation of Planar Four-Link Mechanisms," MTech Thesis, Indian Institute of Technology, Kanpur, 1997.
- [2] Hain, K., "Applied Kinematics," McGraw-Hill, 1967.
- [3] Tao, D. C., "Applied Linkage Synthesis," Addison-Wesley, 1964.
- [4] Hunt, K. H., "Kinematic Geometry of Mechanisms," Oxford University Press, 1978.
- [5] Erdman, A. G., and Sandor, G. N., "Mechanism Design," Vol. I and II, Prentice Hall, 1991.
- [6] Mallik, A. K., Ghosh, A., and Dittrich, G., "Kinematic Analysis and Synthesis of Mechanisms," CRC Press, 1994.
- [7] Hartenberg, R. S., and Denavit, J., "Kinematic Synthesis of Linkages," McGraw-Hill, 1964.
- [8] McLarnan, C. W., "Synthesis of Six Link Plane Mechanisms by Numerical Analysis." *Journal of Engineering for Industry*, Feb. 1963, pp. 5-11.
- [9] Fox, R. L., and Gupta, K. C., "Optimization Technology as Applied to Mechanism Design," *Journal of Engineering for Industry*, Feb. 1975, pp. 657-63.

- [10] Bagci, C., "Optimum Synthesis of Planar Function Generators by the Linear Partition of the Dyadic Loop Equations," *Mechanism and Machine Theory*, Vol. 11, 1976, pp. 33-46.
- [11] Bagci, C., and Jack In - Ping Lee, "Optimum Synthesis of Plane Mechanisms for the Generation of Paths and Rigid-Body Positions via the Linear Superposition Technique," *Journal of Engineering for Industry*, Feb. 1975, pp. 340-6.
- [12] Bagci, C., "Optimum Synthesis of Multiloop Planar Mechanisms for Function Generation via the Linear Superposition Technique," *Proc. I. Mech. E.*, Vol. 189, 1975, pp. 855-9.
- [13] Bagci, C., and Bhatia, D. H., "Optimum Synthesis of Multiloop Planar Mechanisms for the Generation of Paths and Rigid-Body Positions via the Linear Partition of Design Equations," *Journal of Engineering for Industry*, Feb. 1977, pp. 116-23.
- [14] Deb, K., "Optimization for Engineering Design," Prentice-Hall of India, 1995.
- [15] Shukla, G., and Mallik, A. K., "Detection of a Crank in Six-Link Planar Mechanisms," Sent for Publication.
- [16] Lafore, R., "OOP in TURBO C++," Galgotia Publications Pvt. Ltd.. New Delhi. 1996.

Appendix A

The kinematic analysis of a linkage gives its performance characteristics. The analysis deals with the displacement, velocity and acceleration of the member links.

The software package provides the following facilities for the kinematic analysis of a six-bar linkage:

1. Displacement analysis: For the specified dimensions and input movement of a linkage, the movements of all other links are obtained. The ranges of angular displacements of all the links can also be seen.
2. Velocity analysis: The angular velocity of any link (for a prescribed input) is obtained both in tabular and graph forms.
3. Acceleration analysis: The package also gives the complete acceleration analysis of the linkage.

The analysis is based on the analytical method of differentiating the loop closure equations of the linkage with respect to time. The details of the method can be referred to in [6].

Apart from these facilities, transmission angle curves can also be obtained. Provision for kinematic inversion is present by allowing the user to change the fixed link of the linkage. Coupler curves drawn by a specified point on the floating link can be obtained. This gives insight to the path behavior of the coupler point.